Biogeochemical processes captured by carbon isotopes in redox-stratified water columns: a comparative study of four modern stratified lakes along an alkalinity gradient.

Robin Havas[a,*], Christophe Thomazo[a,b], Miguel Iniesto[c], Didier Jézéquel[d], David Moreira[c], Rosaluz Tavera[e], Jeanne Caumartin[f], Elodie Muller[f], Purificación López-García[c], Karim Benzerara[f]

[a] Biogéosciences, CNRS, Université de Bourgogne Franche-Comté, 21000 Dijon, France

[b] Institut Universitaire de France, 75005 Paris, France

[c] Ecologie Systématique Evolution, CNRS, Université Paris-Saclay, AgroParisTech, 91190 Gif-sur-Yvette, France

[d] IPGP, CNRS, Université de Paris, 75005 Paris, and UMR CARRTEL, INRAE & USMB, France

[e] Departamento de Ecología y Recursos Naturales, Universidad Nacional Autónoma de México, México

[f] Sorbonne Université, Muséum National d'Histoire Naturelle, CNRS, Institut de Minéralogie, de Physique des Matériaux et de Cosmochimie (IMPMC), 75005 Paris, France.

[*] *Correspondence to*: Robin Havas (robin.havas@gmail.com)

Keywords: Carbon cycle; DIC; POC; isotopic fractionation; Precambrian analogues

Abstract. Redox-stratified water columns are a prevalent feature of Earth history, and ongoing environmental changes tend to promote a resurgence of such settings. Studying modern redox-stratified environments has improved our understanding of biogeochemical processes and element cycling in such water columns. These settings are associated with peculiar carbon biogeochemical cycling owing to a layered distribution of biological processes in relation to oxidant availability. These processes and their sedimentological expression, notably inferred from paired organic matter–carbonate isotopic compositions of carbon, can vary from one stratified environment to another, because metabolisms from different biogeochemical layers are diverse and may differently imprint the sedimentological record. This variability can arise from numerous physico-chemical parameters, such as sedimentation rate, pH, trace element availability, or basin physiography. Changes in the organic/inorganic carbon sources and mass balance can further complicate the isotopic message in these systems. Better understanding of these multifaceted carbon isotope signals requires further evaluation of the transfer function from the processes occurring in redox-stratified water columns to sediments. We therefore characterized and compared the isotopic signatures of carbonate, organic matter, and dissolved inorganic carbon (DIC) reservoirs at different depths in the water column and upper sediments of four stratified Mexican lakes that follow a gradient of alkalinity/salinity. Comparing these systems shows strong diversity in both the water column and sedimentary carbon isotope signals. Differences in inorganic carbon isotope signatures arise primarily from the size of the DIC reservoirs, buffering the expression of redox-dependent biological processes as alkalinity increases. Combining this isotopic dataset with physico-chemical parameters of the water columns allows us to identify the activity of oxygenic photosynthesis and aerobic respiration in the four lakes studied, while anoxygenic photosynthesis is evidenced in two of them. However, sedimentary organic matter does not originate from the same water column layers in the four lakes, highlighting the ecological variability that can stem from distinct stratified water columns and how it is transferred to the sedimentary record. The least alkaline lake shows higher isotopic variability, and signatures typical of methanogenesis in the sediment porewaters. This metabolism, however, does not leave diagnostic isotopic signatures in the sedimentary archives (organic matter and carbonates), underlining the fact that even when alkalinity does not strongly buffer the inorganic carbon reservoir, a comprehensive picture of the active biogeochemical carbon cycling is not necessarily transferred to the geological record.

1. INTRODUCTION

The carbon cycle and biogeochemical conditions prevailing at the surface of the Earth are intimately bound through biological (e.g. photosynthesis) and geological processes (e.g. volcanic degassing and silicate weathering). The analysis of carbon isotopes in organic matter and carbonates ($\delta^{13}C_{org}$ and $\delta^{13}C_{carb}$) in the rock record, has been used to reconstruct the evolution of the biosphere and the oxygenation of the Earth's surface (e.g. Hayes et al., 1989; Karhu and Holland, 1996; Schidlowski, 2001). Coupling $\delta^{13}C_{org}$-$\delta^{13}C_{carb}$ has frequently been used to infer the burial rate of organic C, and thus the redox balance of the atmosphere and hydrosphere (e.g. Karhu and Holland, 1996; Aharon, 2005; Krissansen-Totton et al., 2015; Mason et al., 2017). It has also been used to deduce the presence of metabolisms like anoxygenic chemoautotrophic or methanotrophic bacteria (e.g. Hayes et al., 1999; Bekker et al., 2008; Krissansen-Totton et al., 2015). Coupling $\delta^{13}C_{org}$-$\delta^{13}C_{carb}$ has also been used to discuss oceans stratification and its effect on inorganic and organic C geochemical signatures in sediments (e.g. Logan et al., 1995; Aharon, 2005; Bekker et al., 2008; Ader et al., 2009). Stratification favors the expression and recording of different layers of the water column, with potentially very distinct isotopic signatures. As the oceans were redox-stratified during most of the Earth's history (Lyons et al., 2014; Havig et al., 2015; Satkoski et al., 2015), processes affecting the C cycle were likely different from those occurring in most modern, well-oxygenated environments. This change of conditions could impact the $\delta^{13}C_{org}$ signal at various scales, from changes in diversity and relative abundance of microbial carbon and energy metabolism (e.g. Wang et al., 2016; Iñiguez et al., 2020; Hurley et al., 2021), to larger ecological interactions (e.g. Jiao et al., 2010; Close and Henderson, 2020; Klawonn et al., 2021) and global C dynamics (e.g. Ridgwell and Arndt, 2015; Ussiri and Lal, 2017).

Modern stratified lakes have been used as analogues of ancient redox-stratified systems to better understand the C cycle in the sedimentary isotopic record (e.g. Lehmann et al., 2004; Posth et al., 2017; Fulton et al., 2018). Several number of recent studies have investigated the C cycle in modern stratified water columns (e.g. Crowe et al., 2011; Kuntz et al., 2015; Posth et al., 2017; Schiff et al., 2017; Havig et al., 2018; Cadeau et al., 2020; Saini et al., 2021; Petrash et al., 2022), where many bio-geo-physico-chemical parameters can be directly measured, together with the main C reservoirs. However, investigations of such Precambrian analogues do not necessarily include sediment data, and generally focus on a single environment without integrating views from several systems.

In this study, we measured the concentrations and isotopic compositions of dissolved inorganic carbon (DIC) and particulate organic carbon (POC) throughout the water column of four modern redox-stratified alkaline crater lakes, located in the Trans-Mexican Volcanic Belt (Ferrari et al., 2012).We also measured the concentrations and isotopic compositions of the sedimentary organic carbon and carbonates as well as porewater DIC from surficial sediments (~ 10 cm) at the bottom of the lakes. The four lakes share similar geological and climatic contexts but have distinct solution chemistries along a marked alkalinity–salinity gradient (Zeyen et al., 2021) – as well as distinct planktonic communities (Iniesto et al., 2022). We therefore seek to evaluate how these environmental and ecological differences are recorded in the C isotope signatures in the water columns (DIC–POC) and sedimentary archives (organic matter–carbonates). The four lakes are closed lakes in endorheic basins (Alcocer, 2021; Zeyen et al., 2021), which facilitates the identification of external environmental constraints (e.g. evaporation, C sources) and their influence on processes occurring within the water columns. Depth profiles of the main physico-chemical parameters together with trace and major elements concentrations were measured to pinpoint the dominant biogeochemical processes occurring in the water columns and link them to specific C isotopes signatures.

First, we constrain the main DIC sources and external controls on the lakes' alkalinity. Next, we describe the influence of the inter-lake alkalinity gradient on the inorganic C cycle and stratification of the lakes, and how it is recorded in surficial sediments. Then, by combining POC and DIC data, we identify the sources of organic C to the lakes by describing the main autotrophic reactions occurring in the water columns (e.g. oxygenic and anoxygenic photosynthesis). Finally, we discuss the fate of POC, either recycled (e.g. via methanogenesis) or deposited in the sediments, and how all these processes are recorded (or not) in surficial sediments.

2. SETTING / CONTEXT

2.1. Geology

The four lakes studied here are volcanic maars formed after phreatic, magmatic, and phreatomagmatic explosions, related to volcanic activity in the Trans-Mexican Volcanic Belt (TMVB, Fig. 1). The TMVB originates from the subduction of the Rivera and Cocos plates beneath the North America plate, resulting in a long (~1000 km) and wide (90–230 km) Neogene volcanic arc spreading across central Mexico (Ferrari et al., 2012). The TMVB harbors a large variety of monogenetic scoria cones and phreatomagmatic vents (maars and tuff-cones) as well as stratovolcanoes, calderas, and domes (Carrasco-Núñez et al., 2007; Ferrari et al., 2012; Siebe et al., 2014). Maar crater formation usually occurs when ascending magma meets water-saturated substrates, leading to successive explosions and the excavation of older units (Lorenz, 1986; Carrasco-Núñez et al., 2007; Siebe et al., 2012; Chako Tchamabé et al., 2020).

The first lake, La Alberca de los Espinos (1985 masl), is located at the margin of the Zacapu tectonic lacustrine basin in the Michoacán-Guanajuato Volcanic Field (MGVF) in the central-western part of the TMVB (Fig. 1). It lies on andesitic basement rocks and was dated at ~25 ± 2 ka (Siebe et al., 2012, 2014). The other three lakes (La Preciosa, Atexcac and Alchichica) are all in the same area (~ 50 km²) of the Serdan-Oriental Basin (SOB) in the easternmost part of the TMVB (Fig. 1). The SOB is a closed intra-montane basin at high altitude (~2300 m), surrounded by the Los Humeros caldera to the north and the Cofre de Perote-Citlatépel volcanic range to the east. The basement is composed of folded and faulted Cretaceous limestones and shales, covered by andesitic-to-basaltic lava flows (Carrasco-Núñez et al., 2007; Armienta et al., 2008; Chako Tchamabé et al., 2020). The Alchichica and Atexcac craters was dated at ~ 6-13 ± 5-6 ka (Chako Tchamabé et al., 2020) and 330 ± 80 ka (Carrasco-Núñez et al., 2007), respectively (Table 1). The age of La Preciosa is not known.

2.2. Climate and limnology

La Alberca is a freshwater lake (0.6 psu) with a temperate to semi-humid climate (Rendon-Lopez, 2008; Sigala et al., 2017). In contrast, lakes from the SOB experience a similar temperate to semi-arid climate (Armienta et al., 2008; Sigala et al., 2017). The current climate of the SOB is dominated by dry conditions, reflected by higher evaporation than precipitation fluxes in Lake Alchichica (~ 1686 vs. 392 mm/year; Alcocer, 2021). In La Preciosa, Atexcac, and Alchichica, this trend is reflected by a drop in water level evidenced by the emersion of microbialite deposits (Fig. S1; Zeyen et al., 2021). This evaporation-dominated climate strongly contributes to the relatively high salinity values in these lakes (1.2–7.9 psu), ranging from sub- to hyposaline.

The four lakes are warm monomictic: they are stratified for about nine months of the year, mixing only when thermal stratification breaks down in the cold of winter (Armienta et al., 2008). They are all closed lakes located in an "endorheic" basin (Alcocer, 2021; Zeyen et al., 2021), meaning that they have no inflow, outflow, or connection to other basins through surficial waters such as streams. The only water input is from precipitation and groundwater inflow (quantified for Lake Alchichica; Alcocer, 2021 and references therein).

The four lakes are alkaline (pH ~ 9) but cover a broad range of chemical compositions (including alkalinity, salinity, and Mg/Ca ratio), interpreted as reflecting different concentration stages of an initial alkaline dilute water (Table 1; Zeyen et al., 2021). Variations in concentration stages may be due to differences in climate and, more generally, different hydrological regimes. Microbialite deposits are found in all four lakes (Gérard et al., 2013; Saghaï et al., 2016; Iniesto et al., 2021a, 2021b; Zeyen et al., 2021), and increase in abundance from lower to higher alkalinity conditions (Zeyen et al., 2021).

3. METHOD

3.1. Sample Collection

The sediment core from Lake La Preciosa was collected in May 2016. All other samples were collected in May 2019. The depth profiles of several physico-chemical parameters were measured in the water columns of the four lakes using an YSI Exo 2 multi-parameter probe: temperature, pH, ORP (oxidation reduction potential), conductivity, O_2, chlorophyll a, phycocyanin, and turbidity. Precisions for these measurements were 0.01 °C, 0.1 pH unit, 20 mV, 0.001 mS/cm, 0.1 mg/L, 0.01 µg/L, 0.01 µg/L and 2% FTU unit, respectively. The ORP signal was not calibrated before each profile and is thus used to discuss relative variations over a depth profile. Measurements of the aforementioned parameters served to pinpoint depths of interest for further chemical and isotopic analyses, notably around the redoxcline of the lakes. Water samples were collected with a Niskin bottle. Particulate matter was collected on pre-combusted (2 h at 490°C) and weighted glass fiber filters (Whatman GF/F, 0.7 µm) and analyzed for particulate organic carbon (POC), major and trace elements. Between 1.5 and 5 L of lake water was filtered before the GF/F filters became clogged. The processed solution was filtered again at 0.22 µm with Filtropur S filters (pre-rinsed with lake water filtered at 0.7 µm) for analyses of dissolved inorganic carbon (DIC), and major, minor, and trace ions.

Sediment cores were collected using a 90 mm Uwitec corer close to the deepest point of each lake's water column (Table 1), where anoxic conditions prevail almost all year long. Cores measured between 20 and 85 cm in length. Slices of about 2-3 cm were cut under anoxic conditions, using a glove bag filled with N_2 (anoxia was monitored using a WTW3630 equipped with a FDO O_2 optode). Interstitial porewater was drained out of the core slices using Rhizons in the glove bag. Sediments were transported back to the laboratory within aluminized foils (Protpack, UK). Sediments were then fully dried in a laboratory anoxic N_2-filled glove box.

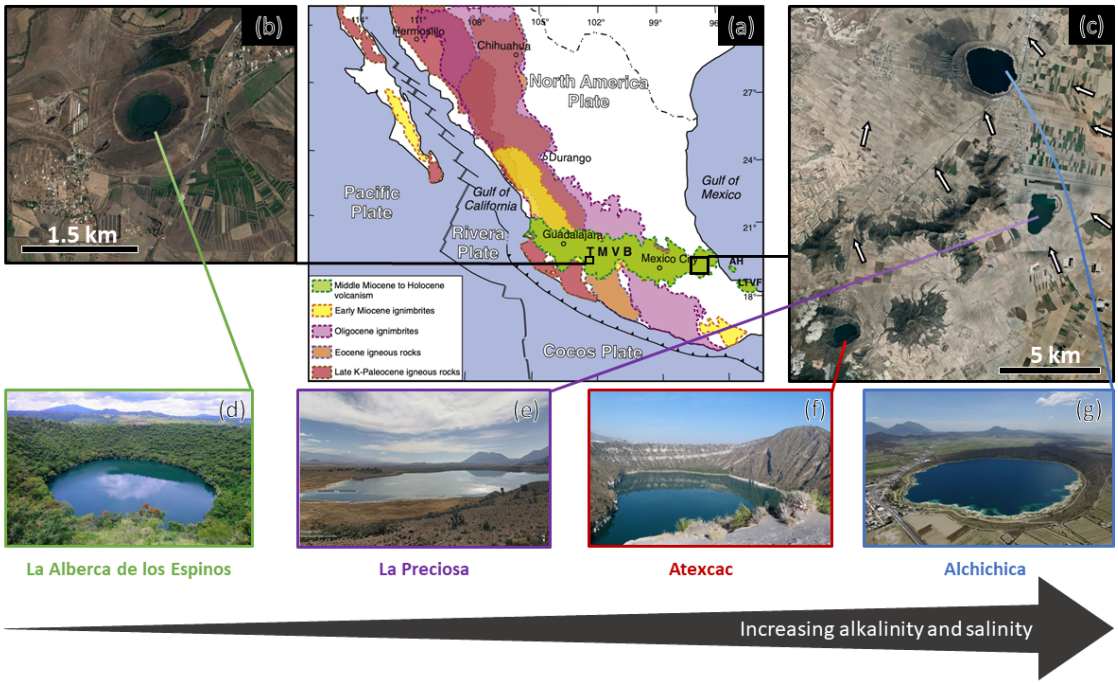

Figure 1. Geographical location and photographs of the four crater lakes. (a) Geological map from Ferrari et al. (2012) with black squares showing the location of the four studied lakes within the Trans-Mexican Volcanic Belt (TMVB). (b, c) Close up © Google Earth views of La Alberca de los Espinos and the Serdan-Oriental Basin (SOB). The white arrows represent the approximate groundwater flow path (based on Silva-Aguilera, 2019). (d-g) Photographs of the four lakes (d from © Google Image ['enamoratedemexicowebsite'], e from © Google Earth street view, and g from © 'Agencia Es Imagen').

Lake	General location	Sampling location	Elevation (masl)
Alchichica	Serdan Oriental Basin, eastern TMVB	19°24'51,5" N; 97°24'09,9" W	2320
Atexcac	Serdan Oriental Basin, eastern TMVB	19°20'2.2'' N; 97°26'59.3'' W	2360
La Preciosa	Serdan Oriental Basin, eastern TMVB	19°22'18.1'' N; 97°23'14.4'' W	2330
La Alberca de los Espinos	Zacapu Basin, MGVF, central TMVB	19°54'23.9'' N; 101°46'07.8'' W	1985

Lake	Lake Basement	Age	Max Depth (m)	Alkalinity (mmoles/L)	Salinity (psu)	pH
Alchichica	limestone, basalts	6-13 ± 5-6 ka	63	~35	7.9	9.22
Atexcac	limestone, andesites, basalts	330 ± 80 ka	39	~26	7.4	8.85
La Preciosa	limestone, basalts	Pleistocene	46	~13.5	1.15	9.01
La Alberca de los Espinos	andesite xenoliths	25 ± 2 ka	30	~7	0.6	9.14

Table 1. General information about the lakes studied. Abbreviations: TMVB: Trans-Mexican Volcanic Belt; MGVF: Michoaćan-Guanajuato Volcanic Field; masl.: meters above sea level. *NB*: Sampling took place in May 2019, except for La Preciosa sediments, sampled in May 2016.

3.2. Dissolved inorganic carbon (DIC) concentration and isotope measurements

Twelve mL of the 0.7-µm filtered lake water was filtered at 0.22-µm directly into hermetic Exetainer® tubes to avoid exchange between DIC and atmospheric CO_2. The DIC concentrations and isotopic compositions were measured at the Institut de Physique du Globe de Paris (IPGP, France), using an Analytical Precision 2003 GC-IRMS, running under He-continuous flow, following the protocol described by Assayag et al. (2006). A given volume of the solution was extracted from the Exetainer® tube with a syringe, while the same volume of helium was introduced to maintain stable pressure and atmospheric-CO_2-free conditions within the sample tubes. The collected sample was inserted into another Exetainer® tube, pre-filled with a few drops of 100% phosphoric acid (H_3PO_4) and pre-flushed with He gas. Under acidic conditions, DIC quantitatively converts to gaseous and aqueous CO_2, which equilibrates overnight within the He-filled head space of the tube. Quantification and isotopic analyses of released gaseous CO_2 were then carried out by GC-IRMS using internal standards of known composition that were prepared and analyzed via the same protocol. Each measurement represented an average of four injections in the mass spectrometer. Chemical preparation and IRMS analysis were duplicated for all the samples. The $\delta^{13}C_{DIC}$ reproducibility calculated for the 65 samples was better than ±0.2 ‰, including internal and external reproducibility. Standard deviation for [DIC] was 0.6 ± 0.9 mmol/L on average.

Specific DIC speciation, i.e., $CO_{2(aq)}$, HCO_3^- and CO_3^{2-} activities, was computed using Phreeqc with the full dissolved chemical composition of each sample as an input. It should be noted that these results are calculated from theoretical chemical equilibria and do not necessarily take into account local kinetic effects, which, for example, could lead to local exhaustion of $CO_{2(aq)}$ where intense photosynthesis occurs.

3.3. Particulate organic carbon and nitrogen (POC / PON)

Particulate organic matter from the lake water columns was collected on GF/F filters, dried at room temperature and ground in a ball mill before and after decarbonation. Decarbonation was performed with 12N HCl vapors in a desiccator for 48 h. Aliquots of dry decarbonated samples (25 - 70 mg) were weighed in tin capsules. The POC and PON contents and $\delta^{13}C_{POC}$ were determined at the Laboratoire Biogéosciences (Dijon, France) using a Vario MICRO cube elemental analyzer (Elementar, Hanau, Germany) coupled in continuous flow mode with an IsoPrime IRMS (Isoprime, Manchester, UK). The USGS 40 and IAEA 600 certified materials used for calibration showed reproducibility better than 0.15 ‰ for $\delta^{13}C$. External reproducibility based on triplicate analyses of samples (n=23) was 0.1 ‰ on average for $\delta^{13}C_{POC}$ (1SD). External reproducibility for POC and PON concentrations was 0.001 and 0.005 mmol/L on average, respectively (i.e. 3 and 7 % of measured concentrations).

3.4. Geochemical characterizations of the sediments

Sedimentary organic carbon (SOC), sedimentary organic nitrogen (SON), and their isotopic compositions were measured on carbonate-free residues of the first 12 cm of the sediment cores, produced after overnight 1N HCl digestion. Plant debris (mainly found in La Alberca and Atexcac) was identified upon initial sediment grinding in an agate mortar and analyzed separately. Aliquots of dried decarbonated samples (~ 4-70 mg) were weighed in tin capsules. The SOC and SON contents and $\delta^{13}C$ were determined at the Laboratoire Biogéosciences (Dijon) using

a Vario MICRO cube elemental analyzer (Elementar GmbH, Hanau, Germany) coupled in continuous flow mode with an IsoPrime IRMS (Isoprime, Manchester, UK). The USGS 40 and IAEA 600 certified materials used for calibration had a reproducibility better than 0.2 ‰ for $\delta^{13}C_{SOC}$. Sample analyses (n=67) were at least duplicated and showed an average external reproducibility of 0.1 ‰ for $\delta^{13}C$ (1SD). External reproducibility for SOC and SON contents was 0.1 and 0.03 wt. %, respectively.

Carbon isotope compositions of sedimentary carbonates were analyzed at the Laboratoire Biogéosciences (Dijon) using a ThermoScientific™ Delta V Plus™ IRMS coupled with a Kiel VI carbonate preparation device. External reproducibility was assessed by multiple measurements of NBS19 standard and was better than ± 0.1 ‰ (2σ). Total carbonate concentration was determined by mass balance after decarbonatation for SOC analysis.

Mineralogical assemblages of sediments were determined on bulk powders by X-Ray diffraction (XRD) at the Laboratoire Biogéosciences (Dijon). Samples were ground in an agate mortar. Diffractograms were obtained with a Bruker D8 Endeavor diffractometer with CuKα radiation and LynxEye XE-T detector, under 40 kV and 25 mA intensity. Mineral identification was based on COD ("Crystallography Open Database") and BGMN databases. Mineral abundances were estimated by Rietveld refinement analysis implemented in the Profex software.

Solid sulfide concentrations were determined on dry bulk sediments from La Alberca Lake after a wet chemical extraction using a boiling acidic Cr(II)-solution as detailed in Gröger et al. (2009).

3.5. Major and trace elements concentrations

Dissolved and particulate matter elemental compositions were measured at the Pôle Spectrométrie Océan (Plouzané, France) by inductively coupled plasma–atomic emission spectroscopy (ICP-AES, Horiba Jobin) for major elements and by high-resolution ICP–mass spectrometry using an Element XR (HR-ICP-MS, Thermo Fisher Scientific) for trace elements. Major element measurement reproducibility based on internal multi-elemental solution was better than 5%. Trace elements were analyzed by a standard-sample bracketing method and calibrated with a multi-elemental solution. Analytical precision for trace elements was generally better than 5%. Dissolved sulfate concentrations were analyzed by ion chromatography at the IPGP (Paris, France) with uncertainty lower than 5%.

4. RESULTS

4.1. Lake La Alberca de los Espinos

Stratification of the water column was well defined in La Alberca de los Espinos (Fig. 2). Temperature was higher than in the other lakes (decreasing from ~23 °C at the surface to 16.5 °C at depth). Dissolved O_2 was oversaturated at the lake surface (118 %, *i.e.*, 7.9 mg/L), rapidly decreasing to 0 between ~ 5 and 12 m, while the oxidation reduction potential (ORP) only decreased below 17 m depth. The offset between O_2 exhaustion and ORP decrease can be explained by the presence of other oxidant species and/or extended chlorophyll a peaks (supplementary text 1). Conductivity decreased from 1.20 to 1.17 mS/cm at 16 m before increasing to 1.27 mS/cm at 26 m (salinity

between 0.58 and 0.64 psu). Chlorophyll a (Chl a) averaged 3.1 µg/L, and showed a profile with at least three distinctive peaks, (i) between 6 and 9.5 m, (ii) around 12.5 m and (iii) between 16 and 19 m, all reaching ~4 µg/L. The turbidity profile showed a pronounced increase from 16 to 19 m. The pH profile showed important variation from 9.15 at the lake surface to 8.75 between 6.5 and 10 m, further decreasing to 7.5 between 16 and 26 m. Based on the temperature profiles, epi-, meta- and hypolimnion layers of Lake La Alberca de los Espinos in May 2019 broadly extended from 0-5, 5-12 and 12-30 m, respectively (Fig. 2). The conductivity and pH profiles, however, show that different conditions prevail at the top and bottom of the hypolimnion.

Dissolved inorganic carbon (DIC) concentration progressively increased from 6.8 mM at 5 m to 8.7 mM at 26 m. The pCO_2 calculated for surface waters was near equilibrium with atmospheric pCO_{2atm}, but strongly increased with depth, up to ~ 40 times the pCO_{2atm} (Table S2). The $\delta^{13}C_{DIC}$ first decreased from about -2.5 ‰ to -4.1 ‰ between 5 and 10 m, before increasing again up to -2 ‰ at 25 m. Particulate organic carbon (POC) concentrations reached minimum values of 0.02 mM at 10 m but rose to maximum values in the hypolimnion (0.06 mM). The C:N molar ratio of particulate organic matter (POM) progressively decreased from 8.5 at the surface to less than 6.5 in the hypolimnion. The $\delta^{13}C_{POC}$ had minimum values at 10 and 17 m (-28.3 and -29 ‰, respectively). Above and below these depths, $\delta^{13}C_{POC}$ averaged -26.4 ± 0.5 ‰.

Dissolved sulfates as measured by chromatography were only detectable at 5 m with a low concentration of 12 µM, while total dissolved S measured by ICP-AES, showed values in the hypolimnion higher than in the upper layers (~ 10.3 vs. 7.4 µM, Table S4). Dissolved Mn concentrations decreased from 1.5 to 0.5 µM between 5 and 10 m, then increased to 2 µM at 25 m. Aqueous Fe was only detectable at 25 m with a concentration of 0.23 µM (Table S4). In parallel, particulate S concentrations increased with depth, with a marked increase from 0.1 to 0.6 µM between 20 and 25m. This was spatially correlated with a 25-fold increase in particulate Fe (from 0.2 to 5.97 µM). Particulate Mn showed a peak between 17 and 20 m around 1 µM, contrasting with values lower than 0.15 µM in the rest of the water column (Fig. 2, Table S5).

In the first centimeters of sediments, DIC concentration in the porewater varied between ~ 11 and 12 mM and $\delta^{13}C_{DIC}$ varied between +8 and +10 ‰ (Figs. 3, 4). Surficial sedimentary carbonates corresponded to calcite and had a $\delta^{13}C$ around -1.5 ‰. Sedimentary organic matter had a $\delta^{13}C_{SOC}$ increasing from ~ -29.4 to -25.5 ‰ and a C:N molar ratio varying between 11.6 and 14.3 (Figs. 3, 4; Table S3).

4.2. Lake La Preciosa

Lake La Preciosa was also stratified at the time of sample collection (Fig. 2). Temperature decreased from ~ 20 °C at the surface to 16 °C at 15m depth. Conductivity showed the same trend with values between 2.24 and 2.22 mS/cm (salinity around 1.15 psu). Dissolved O_2 was oversaturated at the lake surface (120 %, i.e., 8.4 mg/L), rapidly decreasing to 0 between ~ 8 and 14 m, while the ORP decreased right below 16 m. Chl a concentration averaged 3 µg/L and recorded the highest peak compared to the other lakes (about 9 µg/L at 10 m) before decreasing to 0.7 µg/L below 15 m. Turbidity showed a large peak between 16 and 19 m. The pH showed a small decrease from 9 to 8.8 between the surface and 15 m depth. Based on the temperature profiles, epi-, meta- and hypolimnion layers of La Preciosa in May 2019 broadly extended from 0-6, 6-15 and 15-46 m, respectively (Fig. 2).

The DIC concentration was constant throughout the water column at 13.3 mM, with an exception at 12.5 m, where it decreased to 11.5 mM (Fig. 3, Table S1). Calculated pCO_2 at the surface represented about two times the atmospheric pCO_{2atm} (Table S2). The $\delta^{13}C_{DIC}$ decreased from about 0.5 ‰ to -0.36 ‰ between the surface and the hypolimnion. The POC concentration decreased from ~0.06 mM in the epi-/metalimnion to 0.02 mM in the hypolimnion. Similarly, $(C:N)_{POM}$ decreased from ~11.2 in the epi-/metalimnion to 7.6 in the hypolimnion. The $\delta^{13}C_{POC}$ increased downward from ~ -27 to -25 ‰ to with a peak to -23.5 ‰ at 15 m.

In the first 10 cm of sediments, $\delta^{13}C_{SOC}$ values increased downwards from ~ -25.5 to -23.2 ‰ and C:N molar ratio from 9.8 to 11 (Figs. 3, 4; Table S3). Carbonates corresponded to aragonite and calcite and had a bulk C isotope composition averaging 2.6 ‰ (Table S3). Porewaters from the 2016 La Preciosa core were not retrieved.

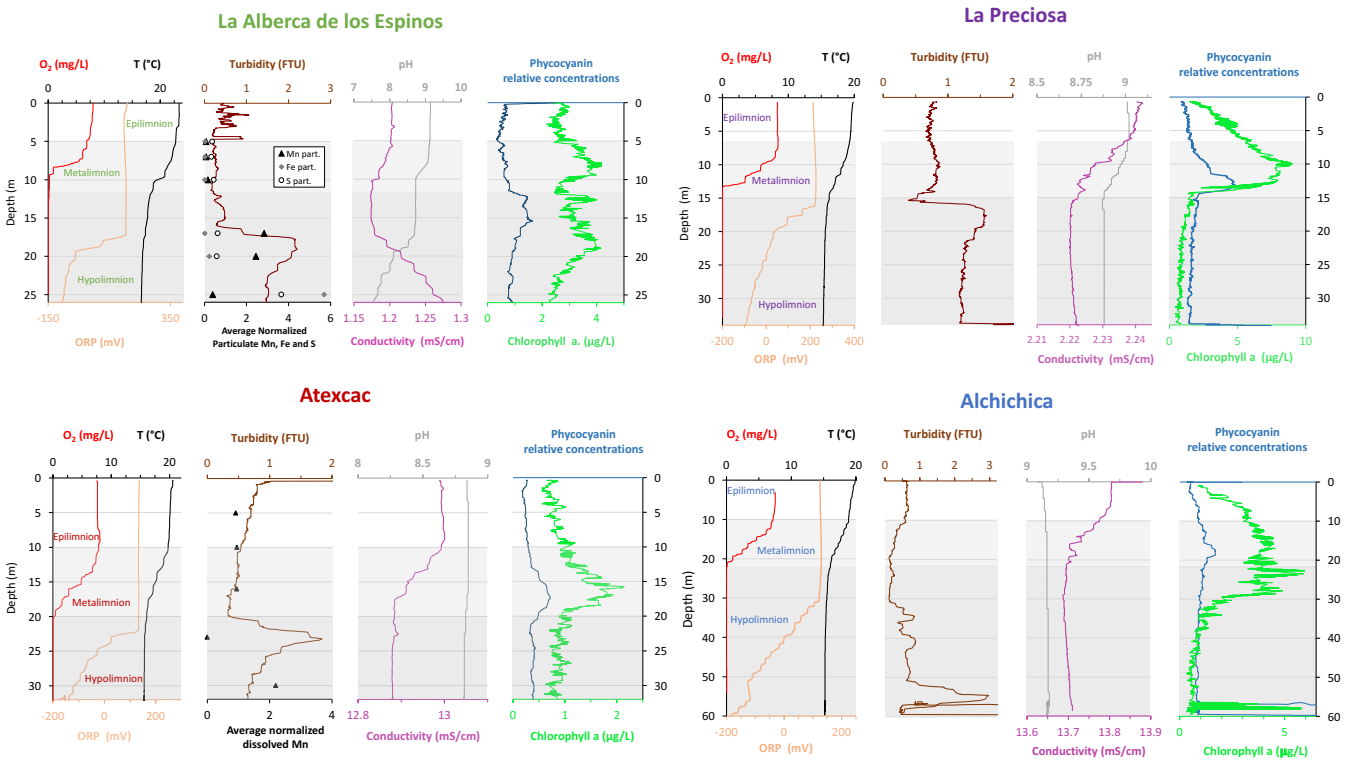

Figure 2. Physico-chemical parameters depth profiles in La Alberca de los Espinos , La Preciosa, Atexcac and Alchichica in May 2019 including: dissolved oxygen concentration (mg/L), water temperature (°C), oxidation-reduction potential (ORP, mV), turbidity (Formazin Turbidity Unit), pH, conductivity (mS/cm), phycocyanin and chlorophyll a pigments (µg/L). Absolute values for phycocyanin concentrations were not determined; only relative variations are represented (with increasing concentrations to the right). Discrete concentration values of dissolved Mn in Atexcac and particulate Mn, Fe and S in La Alberca, normalized by their respective average are represented. Epi-, meta- and hypo-limnion layers are depicted for each lake according to temperature profiles. The three layers closely corresponded to oxygen-rich, oxygen-poor and intermediate zones (except in La Preciosa where the oxycline was slightly thinner than the thermocline layer, ~5 vs. 8 m).

4.3. Lake Atexcac

Stratification of the Lake Atexcac water column was also very well defined (Fig. 2). Temperature decreased from ~ 20.6 °C at the surface to reach 16 °C below 20 m. Conductivity showed the same trend with values between 13 and 12.8 mS/cm near the surface (salinity around 7.4 psu). Dissolved O_2 was slightly oversaturated at the lake

surface (115 % or 7.6 mg/L), rapidly decreasing to 0 mg/L between ~ 10 and 20 m, while ORP signal decreased below a depth of 22 m. Chl a averaged 1 µg/L and showed a narrow peak centered at around 16 m, reaching ~2 µg/L. Turbidity showed a pronounced increase below 20 m, peaking at 23.3 m and returning to surface values at 26 m. The pH remained around 8.85 throughout the water column. Based on the temperature profiles, the epi-, meta- and hypolimnion of Atexcac in May 2019 broadly extended from 0-10, 10-20 and 20-39 m, respectively (Fig. 2).

The DIC concentration was around 26 mM throughout the water column, except at 23 m where it decreased to 24.2 mM (Fig. 3, Table S1). Calculated pCO_2 was about five times higher than the atmospheric pCO_{2atm} (Table S2). The $\delta^{13}C_{DIC}$ was stable around 0.4 ‰ in the epi-/metalimnion, but increased to 0.9 ‰ at 23 m and reached 0.2 ‰ minimum values at the bottom of the lake. The POC concentration was ~ 0.05 mM in the epi-/metalimnion, decreasing to 0.02 mM in the hypolimnion. The C:N molar ratio of POM showed the same depth profile, decreasing from ~9.6 in the epi-/metalimnion to 6.6 in the hypolimnion (Fig. 3). The $\delta^{13}C_{POC}$ showed minimum values in the epi-/metalimnion (-29.3 ‰ at 16 m) and increased to -26.5 ‰ in the hypolimnion.

Dissolved sulfate concentration was relatively stable at ~ 2.51 mM throughout the water column but increased to 2.64 mM at 23 m. Dissolved Mn concentration was constant at 1 µM down to 16 m before dropping to 0 at 23 m, and increasing again to 2.35 µM at 30 m (Fig. 2; Table S4). Similar depth profiles were found for other heavy elements as well, including Cu, Sr, Ba or Pb among others.

In the first 12 cm of sediments, DIC concentration in the porewater varied between ~ 21 and 26 mM, and $\delta^{13}C_{DIC}$ was around 0 ‰. Carbonates corresponded to aragonite and calcite and had a bulk C isotope composition between 2.1 and 2.6 ‰ (Table S3). Sedimentary organic matter had a $\delta^{13}C_{SOC}$ averaging -26.8 ± 0.1 ‰ and a C:N molar ratio increasing from 8 to 10 (Figs. 3, 4; Table S3).

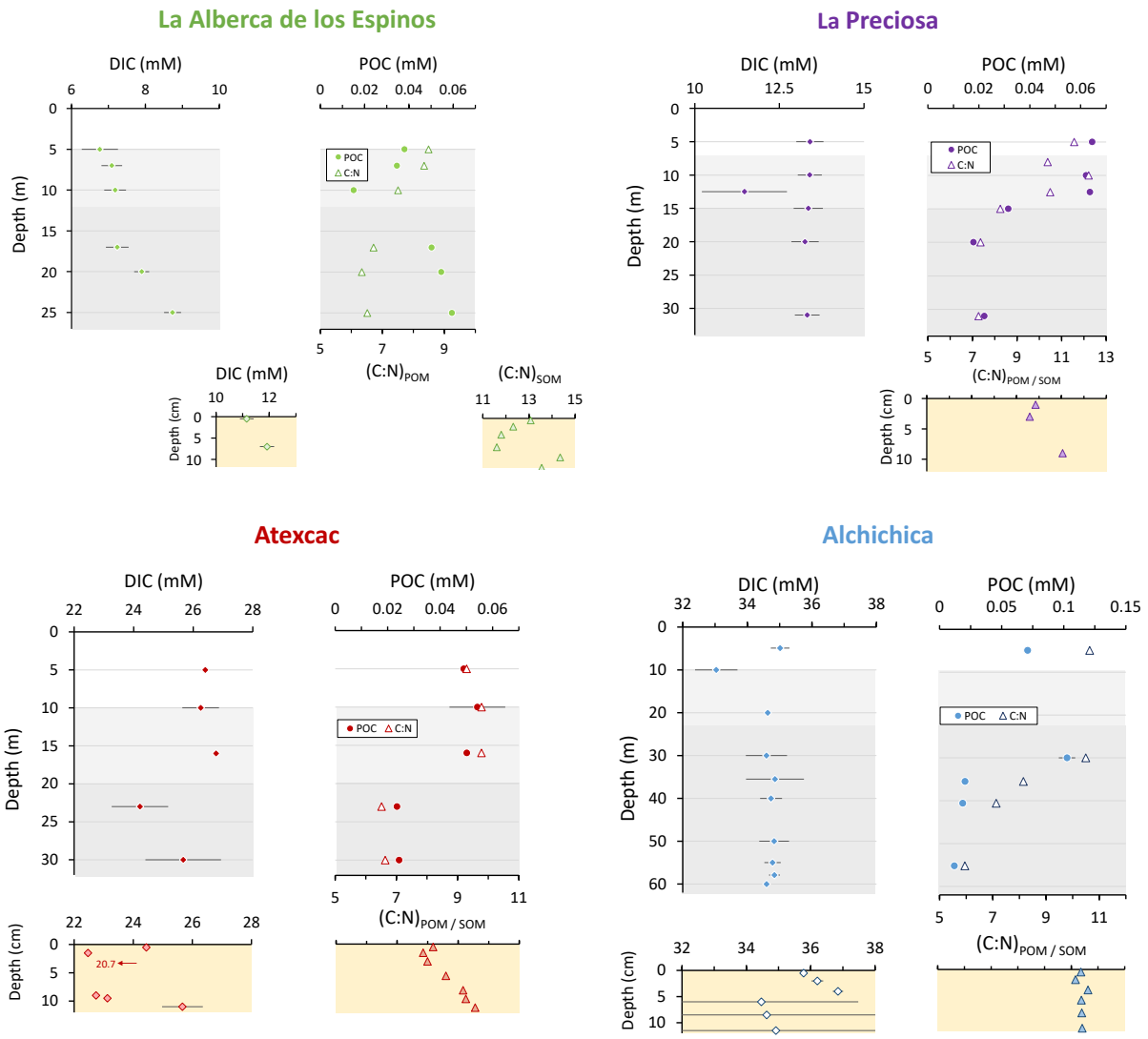

Figure 3. Concentrations in mmol/L (mM) of DIC, DOC, POC and sum of all three reservoirs, C:N molar ratios of POM as a function of depth in the water columns, as well as DIC concentrations in the surficial sediment porewaters and C:N molar ratios of sedimentary OM. Porewaters from La Preciosa's 2016 core were not retrieved.

320

321 **4.4. Lake Alchichica**

322 The water column of Lake Alchichica showed a pronounced stratification compared to previous years at the same
323 period (Fig. 2, Fig. S2; Lugo et al., 2000; Adame et al., 2008; Macek et al., 2020). Temperature decreased from
324 ~ 20 °C at the surface to 15.5 °C at depths below 30 m. Conductivity showed the same trend with values between
325 around 13.8 mS/cm (salinity decreasing from 7.9 to 7.8 psu). Dissolved O_2 was slightly oversaturated at the lake
326 surface (112 % or 7.5 mg/L), rapidly decreasing to 0 mg/L between ~ 10 and 20 m. The ORP followed a similar
327 trend but decreasing below 30 m only. The offset between O_2 exhaustion and decrease of the ORP can be explained
328 by the presence of other oxidant species and/or extended Chl a peaks (supplementary text 1). Chl a averaged
329 2 µg/L, with a broad peak extending from ~ 7 to 29 m (averaging 4 µg/L and showing a narrow 6 µg/L maximum
330 values at 23 m. Then, it decreased to minimum values of ~ 0.5 µg/L in the lower water column. The pH remained

constant at ~9.2 over the whole water column. Based on the temperature profiles, the epi-, meta- and hypolimnion layers of Lake Alchichica in May 2019 extended from 0-10, 10-20 and 20-63 m, respectively (Fig. 2).

The DIC concentration was around 34.8 mM throughout the water column, except at 10 m where it decreased to 33 mM (Fig. 3; Table S1). Calculated pCO_2 was about three times higher than the atmospheric pCO_{2atm} (Table S2). The $\delta^{13}C_{DIC}$ decreased from 2 to ~ 1.5 ‰ between 5 and 60 m depth (Fig. 4; Table S1). The POC concentration was ~ 0.09 mM in the epi-/metalimnion, decreasing to 0.02 mM in the hypolimnion. The $\delta^{13}C_{POC}$ increased from -26.5 ‰ in the top 30 m to -24.1 ‰ at 55 m. The C:N molar ratio of POM showed a similar profile with values around 10.5 down to 30 m, progressively decreasing towards 5.9 at 55 m (Fig. 3; Table S1).

In the first 12 cm of sediments, porewater DIC had a concentration of ~ 35.5 mM and $\delta^{13}C_{DIC}$ decreased from 0.4 to -0.5 ‰. Solid carbonates were contained within several phases (aragonite, hydromagnesite, huntite and calcite) and had a bulk C isotope composition around 4.6 ‰ (Table S3). Sedimentary organic matter had a $\delta^{13}C_{SOC}$ increasing from -25.7 to -24.5 ‰ and a constant C:N molar ratio slightly higher than 10 (Figs. 3, 4; Table S3).

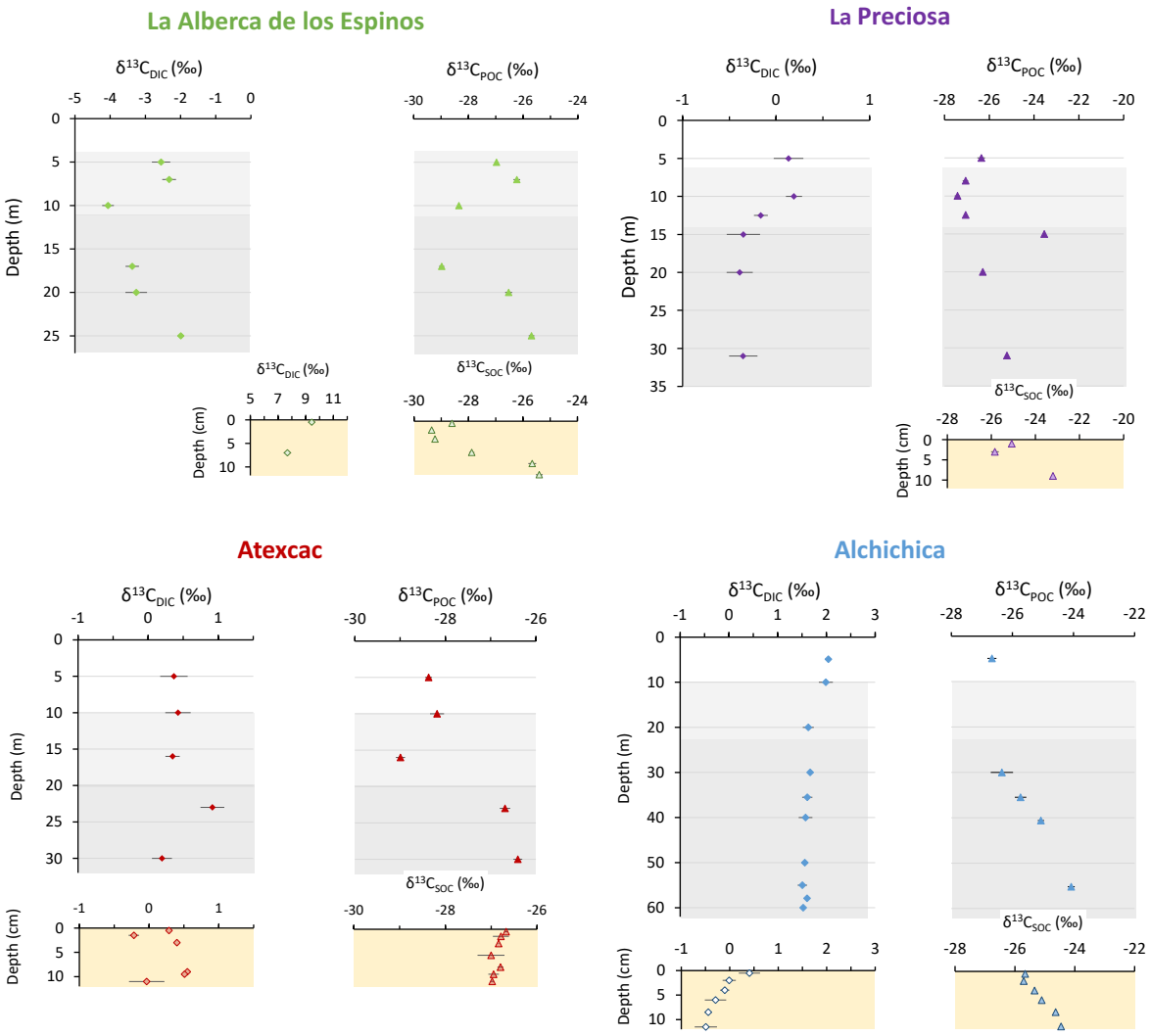

Figure 4. Isotopic compositions of DIC and POC reservoirs as a function of depth in the water columns, as well as isotopic compositions of the porewater-DIC and total organic carbon from the surficial sediments.

5. DISCUSSION

5.1. Inorganic Carbon: origins and implications of the alkalinity/DIC gradient

5.1.1 Sources of DIC and origin of the inter-lake alkalinity gradient

Salinity and DIC concentration gradually increase from La Alberca de los Espinos (0.6 psu, 7 mM) to Alchichica (7.9 psu, 35 mM), while La Preciosa (1.15 psu, 13 mM) and Atexcac (7.44 psu, 26 mM) have intermediate values (Table 1 and S1). This trend matches the alkalinity gradient (with values of ~ 8, 15, 32 and 47 meq/L, Fig. S3a) previously described for these lakes (Zeyen et al., 2021), consistent with the fact that alkalinity is mainly composed of HCO_3^- and CO_3^{2-} ions in most natural waters. This alkalinity gradient may result from different concentration stages of an initial dilute alkaline water (Zeyen et al., 2021), ultimately controlled by differences in hydrological regime between the four lakes. In the SOB, the weathering of basaltic/andesitic bedrock (Armienta et al., 2008; Carrasco-Núñez et al., 2007; Lelli et al., 2021) and Cretaceous limestone (with $\delta^{13}C \approx 0 \pm 1$ ‰; Gonzales-Partida et al., 1993; Armstrong-Altrin et al., 2011) favors the inflow of more alkaline and DIC-concentrated groundwater than in La Alberca, which lies on an essentially basaltic basement (Rendon-Lopez, 2008; Siebe et al., 2014; Zeyen et al., 2021). The SOB is currently experiencing higher rates of evaporation than precipitation (Alcocer, 2021), which may play an important role in concentrating solutes and decreasing the water level in La Preciosa, Atexcac, and Alchichica (Anderson and Stedmon, 2007; Zeyen et al., 2021). Substantial "sub-fossil" microbialite deposits emerge well above the current water level in lakes Atexcac and Alchichica, confirming this fall in water level (~15 m for Atexcac, and ~5 m for Alchichica). Scattered patches of microbialites emerge at La Preciosa (suggesting a water level decrease of ~6 m). By contrast, emerged microbialites are virtually absent in Lake La Alberca de los Espinos (Fig. S1).

Additional local parameters such as variable groundwater paths and fluxes (Furian et al., 2013; Mercedes-Martín et al., 2019; Milesi et al., 2020; Zeyen et al., 2021) most likely play a role in explaining some of the variation in DIC concentration between lakes. La Preciosa's water composition significantly differs from that of Atexcac, and Alchichica, despite a similar geological context and climate (all are located within 50 km^2, Fig. 1). Groundwater in the SOB area becomes more saline as it flows towards the center of the basin and through the crater lakes (Silva Aguilera, 2019; Alcocer, 2021). Since groundwater flows through La Preciosa first, it becomes more concentrated as it enters Alchichica (Silva Aguilera, 2019; Alcocer, 2021; Lelli et al., 2021). Different regimes of volcanic CO_2 degassing into these crater lakes may also contribute to variation in the C mass balance and $\delta^{13}C_{DIC}$ values between the four lakes. Near the lakes from the SOB area, geothermal fluids derived from meteoric waters have been shown to interact with deep volcanic fluids as well as the calcareous basement rocks (Peiffer et al., 2018; Lelli et al., 2021). In the water column of La Alberca, $\delta^{13}C_{total}$ averages -4.8 ‰ (Havas et al., submitted). This isotopic composition is very similar to signatures of mantle-CO_2 (Javoy et al., 1986; Mason et al., 2017), which could buffer the overall C isotope composition of this lake. La Alberca is located on top of a likely active normal fault (Siebe et al., 2012), favoring the ascent of volcanic gases.

Differences in the remineralization rate of organic carbon (OC) could also contribute to the heterogeneous DIC content among the lakes. However, assuming that all OC from the lakes ultimately remineralized into DIC, it would still represent only a small proportion of the total carbon (9 % for La Alberca, ~5 % for La Preciosa and Alchichica, and 16 % for Atexcac, Havas et al., submitted). From an isotopic mass balance perspective, Lake La

Alberca exhibits more negative $\delta^{13}C_{DIC}$ (and $\delta^{13}C_{Carb}$), slightly closer to OC signatures, whereas the $\delta^{13}C_{DIC}$ of the three SOB lakes lie very far from OC isotopic signatures (Fig. 4). Dense vegetation surrounds La Alberca (Fig. S1), making it the only lake in this study where OC respiration could be a significant source of inorganic C to the water column (potentially influencing the P_{CO2}, [DIC] and pH profiles described above).

In summary, a combination of very local and external environmental factors generates the contrasting water chemistries of the lakes, notably a gradient in their alkalinity/[DIC]. This variability stems from the exact nature of the basement rocks, the distinct groundwater flow paths feeding the lakes, differences in evaporation rates, and potentially different volcanic-CO_2 degassing regimes.

5.1.2 Influence of alkalinity on physico-chemical stratification in the four lakes

Stratified water columns can sustain strong physico-chemical gradients, where a wide range of biogeochemical reactions impacting the C cycle can take place (e.g. Jézéquel et al., 2016). In the four lakes studied here, the evolution of pH with depth exemplifies the interplay between the alkalinity gradient, the physico-chemical stratification of the lakes, and their respective C cycle. The pH shows a stratified profile in La Alberca and La Preciosa, but remains constant in Atexcac and Alchichica. The decline in pH at the oxycline of La Preciosa is associated with the decrease in POC and chlorophyll a concentrations and $\delta^{13}C_{DIC}$ values, reflecting the impact of oxygen respiration (i.e. carbon remineralization) at this depth (Figs. 2-4). In La Alberca, the surface waters are markedly more alkaline than the bottom waters, with a two-step decrease in pH occurring at 8 m and 17 m (with a total drop of 1.5 pH unit). As in La Preciosa, this likely results from high OM respiration, although input of volcanic acidic gases (e.g. dissolved CO_2 with $\delta^{13}C \sim -5$ ‰) might also contribute to the pH decrease in the bottom waters, reflected by negative $\delta^{13}C_{DIC}$ signatures and an increase of [DIC] and conductivity in the hypolimnion (Figs. 2 and 4). By contrast, while the same evidence for oxygen respiration ([POC], chlorophyll a) can be detected in the other two lakes, it does not impact their pH profile in a similar way (Fig. 2). This result suggests that the acidity generated by these reactions is buffered by the much higher alkalinity measured in these two lakes.

External forcings such as lake hydrology and fluid sources thus impact the alkalinity buffering capacity of these lakes and influence the vertical pH profile of the water columns. This is particularly important considering the critical interplay between pH and biogeochemical reactions affecting the C cycle (e.g. Soetaert et al., 2007).

5.1.3 Sinks of DIC along the alkalinity gradient

Interplay between pH and sources of alkalinity/DIC in the lakes also has a strong impact on their C storage capacity as it can result in different fluxes of the C sinks (inorganic and organic C precipitation / sedimentation, CO_2 degassing).

Alkaline pH can store large quantities of DIC because it favors the presence of HCO_3^- and CO_3^{2-} species over H_2CO_3* (the intermediate species between gaseous $CO_{2(g)}$ and bi-/carbonate ions, defined here as the sum of H_2CO_3 and $CO_{2(aq)}$). Carbonate and bicarbonate ions represent over 99% of total DIC in the four lakes (Table S2). In La Alberca de los Espinos, the lake with the lowest DIC, the surface water pCO_2 is slightly lower than atmospheric

420 pCO_{2atm} (Table S2). By contrast, large amounts of CO_2 degas at the surface of the SOB lakes, as indicated by their
421 elevated surface water pCO_2, from 2 to 5 times higher than atmospheric pCO_{2atm} (Table S2). These observations
422 are consistent with the notion that higher DIC concentrations favor CO_2 degassing through higher pCO_2 (e.g.
423 Duarte et al., 2008). Although La Alberca and Alchichica (the two endmembers of the alkalinity gradient) have
424 the same surface water pH, CO_2 degassing is three times higher at Alchichica, for a given value of gas transfer
425 velocity.

426 Another important C sink for these lakes is the precipitation of carbonate minerals, found in the microbialites and
427 lake sediments. Lake alkalinity and resulting mineral saturation index greatly influence the amount of C
428 precipitated from the lake waters. Although the four lakes are supersaturated with aragonite, calcite and the
429 precursor phase monohydrocalcite, they present highly contrasted amounts of carbonate deposits (Zeyen et al.,
430 2021). The occurrence of microbialites increases along the alkalinity gradient, with limited presence at La Alberca,
431 and more massive deposits at Atexcac and Alchichica (Zeyen et al., 2021; Fig. S1). Similarly, surficial sediments
432 contain only 16 wt. % for La Alberca, but from 40 to 62 wt. % carbonates for the SOB lakes (Table S3). Thus, the
433 SOB lakes seem to bury more C than La Alberca de los Espinos. Nonetheless, the data from May 2019 indicate
434 that La Alberca was the only one of the four lakes with a pCO_2 slightly lower than atmospheric pCO_{2atm}, thus
435 representing a net sink of C. Classifying the three other lakes as net C sources or sinks – notably in order to see
436 the influence of their respective position in the alkalinity gradient – will require a more detailed description of C
437 in- and out-fluxes since they all store and emit significant amounts of C (as organic and inorganic C deposits and
438 via CO_2 degassing, respectively). However, this is out of the scope of the present study.

439

440 **5.1.4 Isotopic signatures of inorganic C in the four lakes ($\delta^{13}C_{DIC}$ and $\delta^{13}C_{Carbonates}$)**

441 The DIC isotopic composition of the lakes (between ~ -3 and +2 ‰ on average; Table S1) is consistent with the
442 DIC sources described above. The lower $\delta^{13}C_{DIC}$ in La Alberca is consistent with influence of remineralized OC
443 and/or volcanic CO_2. The $\delta^{13}C_{DIC}$ in the SOB lakes suggests groundwater $\delta^{13}C_{DIC}$ values resulting from the
444 dissolution of the Cretaceous limestone basement.

445 By controlling DIC speciation ($H_2CO_3/CO_{2(aq)}$, HCO_3^-, CO_3^{2-}), pH also strongly influences $\delta^{13}C_{DIC}$. Indeed, there
446 is a temperature-dependent fractionation of up to 10 ‰ between the different DIC species (Emrich et al., 1970;
447 Mook et al., 1974; Bade et al., 2004; Table S6). The Mexican lakes present $\delta^{13}C_{DIC}$ values that are common for
448 lakes with a pH around 9 (Bade et al., 2004), where DIC is dominated by HCO_3^-. However, the pH values of the
449 four lakes studied here are too similar to explain the significant difference between their $\delta^{13}C_{DIC}$ (Fig. 4; p=4.2x10^{-3}
450 for La Preciosa and Atexcac, which have the closest $\delta^{13}C_{DIC}$). Part of the variability of $\delta^{13}C_{DIC}$ among the lakes
451 may result from their distinct evaporation stages, as the mean $\delta^{13}C_{DIC}$ values of the lakes broadly correlate with
452 their salinity/alkalinity (Fig. S3b). Evaporation generally increases the $\delta^{13}C_{DIC}$ of residual waters by increasing
453 lake pCO_2 and primary productivity. This bolsters CO_2 degassing and organic C burial, which have low $\delta^{13}C$
454 compared to DIC (e.g. Li and Ku, 1997; Talbot, 1990). Accordingly, the pCO_2 of La Alberca is lower than that of
455 the other lakes (Table S2). The $\delta^{13}C_{DIC}$ in lakes with lower DIC concentrations is expected to be more easily
456 influenced by exchanges with other carbon reservoirs, such as organic carbon (through photosynthesis/respiration),
457 or other DIC sources (e.g., depleted volcanic CO_2 or groundwater DIC), compared with buffered, high DIC lakes

(Li and Ku, 1997). As a result, the low DIC/alkalinity concentration in La Alberca features the lowest $\delta^{13}C_{DIC}$ of the four lakes, likely reflecting organic and/or volcanic C influence and thus higher responsiveness to biogeochemical processes of the inorganic C reservoir. By contrast, the three SOB lakes exhibit $\delta^{13}C_{DIC}$ with less internal variability, with a maximum amplitude of 0.7 ‰ within a single water column.

Surficial sedimentary carbonates are in isotopic equilibrium with the $\delta^{13}C_{DIC}$ of the water columns, within the uncertainty of $\delta^{13}C_{DIC}$ measurement, and more specifically with the $\delta^{13}C_{DIC}$ values at the oxycline/thermocline of the lakes (Tables S6 and S7). This is estimated by correcting the carbonates C isotope composition ($\delta^{13}C_{Carb}$) by the fractionation value between DIC and the different carbonate mineralogies (supplementary text S2). Therefore, the $\delta^{13}C_{Carb}$ also follows and reflects the alkalinity gradient, with the lowest $\delta^{13}C_{Carb}$ found in the surficial sediments of La Alberca (~ -1.5 ‰), intermediate values in La Preciosa and Atexcac (~2.5 ‰), and the highest values in Alchichica (~ +4.6 ‰) (Table S3).

In summary, although all four lakes present the same general structure and environmental conditions (i.e. tropical alkaline stratified crater lakes), external and local factors (e.g. hydrology, fluid sources, and stratification characteristics) result in contrasting water chemistry compositions, which have a critical impact on the physico-chemical depth profiles of each lake and their biogeochemical carbon cycle functioning. These external factors represent a first-order control on the size, isotopic composition, and responsiveness to biogeochemical processes of the inorganic C reservoir. Lakes with the highest alkalinity/DIC content will poorly record internal biological processes. Interestingly, C storage in mineral carbonates seems to be significant in watersheds where carbonate deposits pre-exist in the geological substratum (here, the Cretaceous limestone basement), providing more alkaline and C-rich sources.

Symbols	Mathematical Expression	Signification
$\delta^{13}C_X$	$\left(\frac{\left(\frac{^{13}C}{^{12}C}\right)_X}{\left(\frac{^{13}C}{^{12}C}\right)_{\dots\dots}} - 1\right) * 1000$	Relative difference in ^{13}C:^{12}C isotopic ratio between a sample of a given C reservoir and the international standard "Vienna Pee Dee Bee", expressed in permil (‰). $\delta^{13}C_{total}$ represents the weighted average of $\delta^{13}C$ for all DIC and POC.
$\Delta^{13}C_{X\text{-}Y}$	$= \delta^{13}C_X - \delta^{13}C_Y \approx 1000 ln \alpha_{X\text{-}Y}$	Apparent isotopic fractionation between two reservoirs 'X' and 'Y'. Difference between their measured C isotope compositions approximating the fractionation α in ‰.
$\varepsilon_{X\text{-}CO2}$	$= (\alpha_{X\text{-}CO2} - 1)1000 \approx \delta^{13}C_X - \delta^{13}C_{CO2}$	Calculated isotopic fractionation between a reservoir 'X' and $CO_{2(aq)}$. $\alpha_{X\text{-}CO2}$ is calculated as $(\delta^{13}C_X+1000)/(\delta^{13}C_{CO2}+1000)$ where $\delta^{13}C_X$ is measured and $\delta^{13}C_{CO2}$ is computed based on DIC isotopic composition and speciation (see supplementary text S3).

Table 2

Index for mathematical notations used in the text including C isotopic composition of a reservoir X ($\delta^{13}C_X$), isotopic discrimination between the two carbon reservoirs X and Y ($\Delta^{13}C_{X\text{-}Y}$). In the main text, we report organic C isotope discrimination *versus* both bulk DIC ($\Delta^{13}C_{POC\text{-}DIC}$) – in a way to facilitate studies intercomparison and because it is the commonly reported raw measured data (Fry, 1996) – and calculated $CO_{2(aq)}$ ($\varepsilon_{POC\text{-}CO2}$) in order to discuss the intrinsic isotopic fractionations associated with the lakes metabolic diversity. All C isotope values and fractionations are reported relative to the international standard VPDB (Vienna Pee Dee Belemnite).

5.2. Particulate organic carbon: from water column primary production to respiration recycling and sedimentary organic matter

5.2.1. Particulate organic C sources

Primary productivity by oxygenic photosynthesis in the upper water column

All four crater lakes are endorheic basins, with no surface water inflow or outflow. The organic carbon sources are therefore predominantly autochthonous, resulting mainly from planktonic autotrophic C fixation. This is supported by C:N ratios of POM that ranged from 6 to 12 in the four lakes, close to the phytoplankton Redfield but far from land plant ratios. Abundant vegetation covers the crater walls of La Alberca and to a lesser extent those of Atexcac; some plant debris was observed and sampled from the sediment cores of these two lakes. They have high C:N ratios (between 24 and 68), typical of plant tissues and significantly higher than those of the bulk organic matter in the surficial sediments (between 8 and 13) and water column (between 6 and 12) (Fig. 3). Thus, the allochthonous organic carbon in these two lakes does not significantly contribute to their bulk organic signal.

The importance of planktonic autotrophic C fixation as a major source of POC in the four lakes is further supported by the assessment of the isotopic discrimination between DIC and organic biomass, expressed as $\Delta^{13}C_{POC\text{-}DIC}$ and $\varepsilon_{POC\text{-}CO2}$ (Table 2). The $\Delta^{13}C_{POC\text{-}DIC}$ varies between ~ -29 and -23 ‰ (corresponding to $\varepsilon_{POC\text{-}CO2}$ between ~ -19 and -13 ‰) throughout the four water columns, within the typical range of planktonic oxygenic phototrophs (Pardue et al., 1976; Sirevag et al., 1977; Thomas et al., 2019). Yet these values exhibit variability – both within a single water column (up to 4.5 ‰) and among the four lakes (up to 6 ‰, Figs. 4 and 5). This variability may reflect several abiotic and biotic factors.

Notably, lower DIC availability in La Alberca and La Preciosa probably makes the carboxylation step less limiting during photosynthesis (e.g. O'Leary, 1988; Descolas-Gros and Fontungne, 1990; Fry, 1996), decreasing $|\varepsilon_{POC\text{-}CO2}|$ in these lakes (between 14.5 and 17.7 ‰ at the peak of Chl. a) compared with Atexcac and Alchichica (Fig. 5a; between 17.5 and 19.2 ‰). Lower $CO_{2(aq)}$ availability and/or higher reaction rates result in transport-limited rather than carboxylation-limited fixation, with smaller C isotope fractionation between POC and DIC (Pardue et al., 1976; Zohary et al., 1994; Fry, 1996; Close and Henderson, 2020). The isotopic fractionation associated with diffusion is much smaller than with carboxylation, and a higher proportion of the DIC entering the cells is converted into organic biomass (e.g. Fogel and Cifuentes, 1993). We consistently notice a correlation among the

lakes between $a(CO_2)_{(aq)}$ (or [DIC]) and $|\varepsilon_{POC\text{-}CO2}|$ at depths where oxygenic photosynthetic peaks (Fig. 6). Furthermore, La Alberca and La Preciosa are considered less oligotrophic than the two other lakes (Lugo et al., 1993; Vilaclara et al., 1993; Havas et al., submitted), with higher chlorophyll a contents and thus smaller $|\varepsilon_{POC\text{-}CO2}|$ (Fig. 5). Higher water temperatures in La Alberca de los Espinos (by ~ 3 °C) could also partly contribute to a smaller $|\varepsilon_{POC\text{-}CO2}|$ in this lake (Sackett et al., 1965; Pardue et al., 1976; Descolas-Gros and Fontungne, 1990).

Unlike $\delta^{13}C_{DIC}$, organic carbon isotope signatures do not evolve linearly with the alkalinity/salinity gradient, suggesting other lake- and microbial-specific controls on these signatures. These controls include: diffusive or active uptake mechanisms, specific carbon fixation pathways, the fraction of intracellular inorganic carbon released out of the cells, cell size and geometry (Werne and Hollander, 2004 and references therein) and remineralization efficiency. Moreover, an increasing amount of isotopic data has evidenced a significant variability of the isotopic fractionation achieved by different purified RuBisCO enzymes ($\varepsilon_{RuBisCO}$, Iñiguez et al., 2020), and even by a single RuBisCO form (Thomas et al., 2019). Thus, caution should be paid to the interpretation of the origin of small isotopic variations of the biomass in distinct environmental contexts because RuBisCO alone can be an important source of this variability (Thomas et al., 2019).

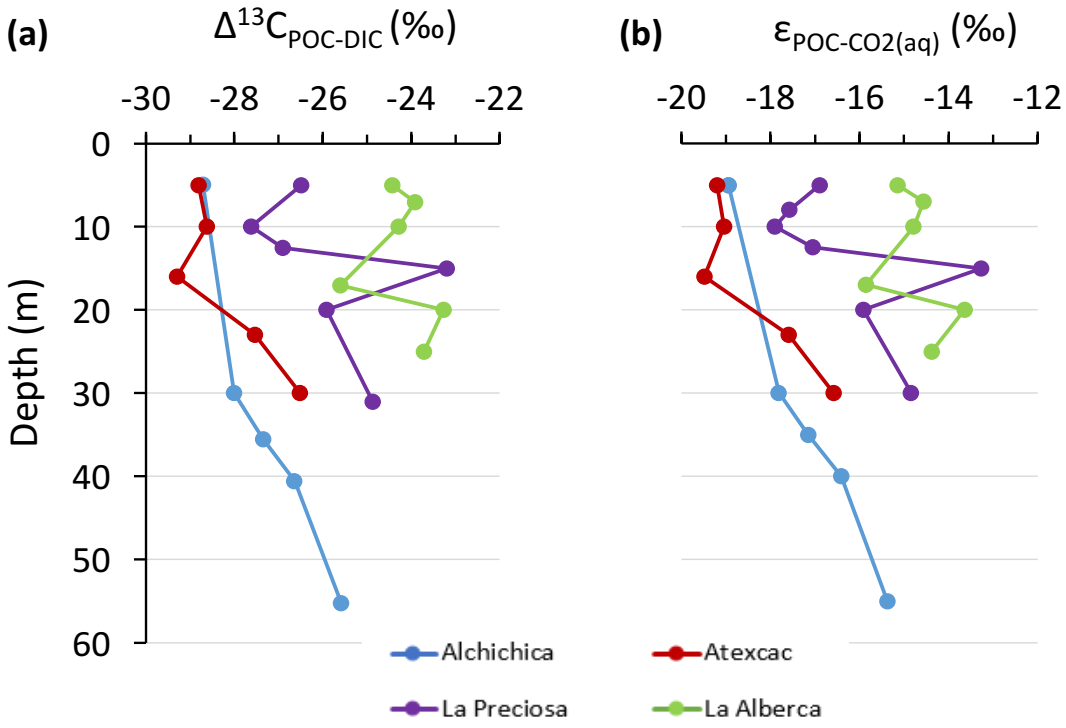

Figure 5. Isotopic fractionations between POC and DIC in the water columns of the four lakes, expressed as a) $\Delta^{13}C_{x\text{-}y}$ and b) $\varepsilon_{POC\text{-}CO2}$. Refer to Table 2 for more detail about the Δ and ε notations.

Primary production in the anoxic hypolimnion

Anoxygenic autotrophs commonly thrive in anoxic bottom waters of stratified water bodies (e.g. Pimenov et al., 2008; Zyakun et al., 2009; Posth et al., 2017; Fulton et al., 2018; Havig et al., 2018). They have been identified at different depths in the four Mexican lakes (Macek et al., 2020; Iniesto et al., 2022). In our samples collected during the stratification period, anoxygenic autotrophs appear to have a distinct impact on the C cycle of La Alberca and Atexcac only. Lake Atexcac records a concomitant decrease in [DIC] and increase in $\delta^{13}C_{DIC}$ in the anoxic hypolimnion at 23 m, below the peak of Chl a, suggesting autotrophic C fixation by chemoautotrophy or anoxygenic photosynthesis. The calculated $\varepsilon_{POC\text{-}CO2}$ at 23 m (-17.3 ‰) is consistent with C isotope fractionation by purple- and green-sulfur-anoxygenic bacteria (PSB and GSB), while $\varepsilon_{POC\text{-}CO2}$ in La Alberca's hypolimnion (~ -15 ‰) is closer to GSB canonical signatures (Posth et al., 2017 and references therein) (Fig. 5b). In La Alberca, anoxygenic primary productivity is suggested by increasing POC concentrations below the oxycline. We also observe a Chl a peak in the anoxic hypolimnion of this lake (Fig. 2), which likely represents a bias of the probe towards some bacteriochlorophyll pigments typical of GSB (see supplementary text S4). In Atexcac, C fixation by anoxygenic autotrophs at 23 m causes a shift in the DIC reservoir, while oxygenic photosynthesis at 16 m does not, suggesting that anaerobic autotrophs are the main autotrophic metabolisms in this lake (in terms of DIC uptake). In La Alberca, the increase in [POC] to maximum values at depth also supports the predominance of anoxygenic *versus* oxygenic autotrophy (Fig. 3). This is similar to other stratified water bodies exhibiting primary production clearly dominated by anoxygenic metabolisms (Fulton et al., 2018).

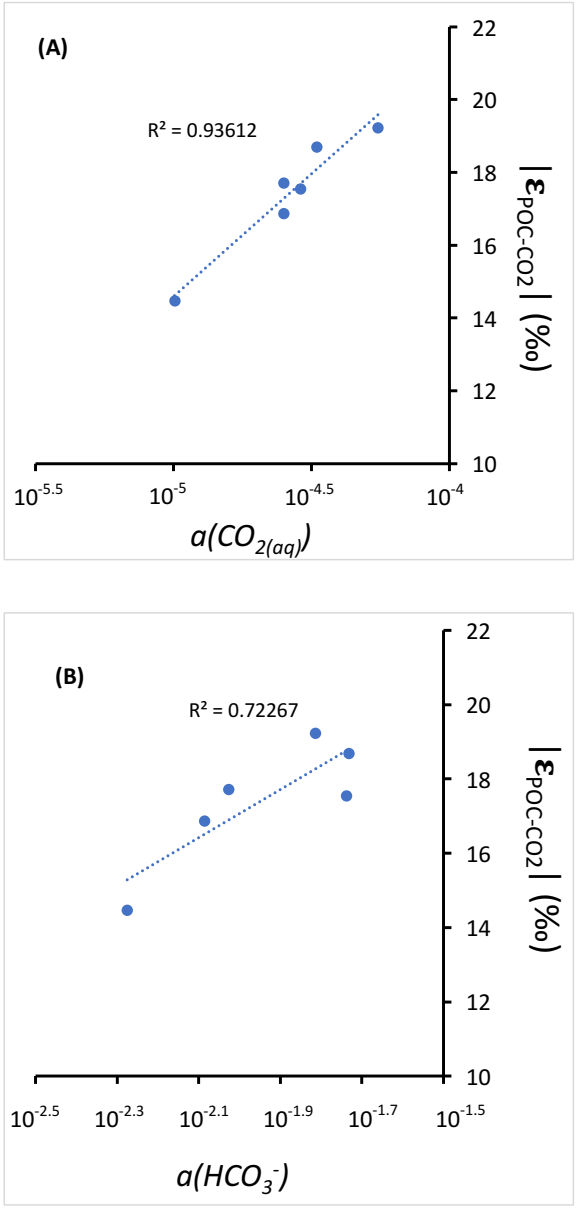

Figure 6.

Cross plots of DIC species activities *versus* absolute values of calculated C isotopic fractionations between POC and CO_2 at depths of peak oxygenic photosynthesis where data was available (5 and 30 m for Alchichica, 16 m for Atexcac, 10 and 12.5 m for La Preciosa and 7 m for La Alberca). (A) Dissolved $CO_{2(aq)}$ activity and (B) bicarbonate activity as functions of $|\varepsilon_{POC\text{-}CO2}|$ in ‰ plus linear correlation trends and corresponding R^2.

Lastly, at 23 m in Atexcac and 17 m in La Alberca, we find a striking turbidity peak precisely where the redox potential and the concentration of dissolved Mn drops (Fig. 2). In Atexcac, the concentration in dissolved metals such as Cu, Pb, or Co also drops at 23 m (Fig. S4). In La Alberca, a peak of particulate Mn concentration is detected at 15 m (Fig. 2; data unavailable for Atexcac). This is most likely explained by the precipitation of Mn mineral particles, where reduced bottom waters meet oxidative conditions prevailing in the upper waters. These oxidized Mn phases can be used as electron acceptors during chemoautotrophy (Havig et al., 2015; Knossow et al., 2015; Henkel et al., 2019; van Vliet et al., 2021). Even at a low particle density, such phases can catalyze abiotic oxidation of sulfide to sulfur compounds, which in turn can be used and further oxidized to sulfate by phototrophic or chemoautotrophic sulfur-oxidizing bacteria (van Vliet et al., 2021). This is also consistent with the small increase in [SO_4^{2-}] observed at 23 m in Atexcac (Table S4).

In summary, combined POC and DIC data allowed us to recognize the most representative autotrophic metabolisms in the Mexican lakes. The upper water columns are all dominated by oxygenic photosynthesis. Lower in the water columns, anoxygenic photosynthesis and/or chemoautotrophy were found to have a noticeable impact on POC and DIC reservoirs in La Alberca and Atexcac only. Their activity was associated with metal elements cycling. More specifically in La Alberca, the anoxygenic phototrophs correspond to GSB.

5.2.2. Sinks of particulate organic carbon: respiration and sedimentation

Aerobic respiration at the oxycline

At the oxycline of stratified water bodies, aerobic respiration of OM by heterotrophic organisms favors the transition from oxygenated upper layers to anoxic bottom waters. In the water column of the four lakes, $\Delta^{13}C_{POC\text{-}DIC}$ (and $\varepsilon_{POC\text{-}CO2}$) show increasing values in the hypolimnion, and especially below the chlorophyll a peaks (Figs. 2 and 5). This trend also correlates with increasing $\delta^{13}C_{POC,}$ decreasing $(C:N)_{POM}$ ratios as well as decreasing POC concentrations except in La Alberca (Figs. 3 and 4). Decreasing POC concentrations near the oxycline and redoxcline are consistent with the fact that part of the upper primary production is degraded deeper in the water columns and/or that there is less primary production in the anoxic bottom waters. Increased $\delta^{13}C_{POC}$ in the hypolimnion of the lakes is consistent with heterotrophic activity and points out that POC at these depths could mainly record secondary production rather than being a residue of sinking degraded OM formed by primary production. Heterotrophic bacteria preferentially grow on available ^{13}C-enriched amino acids and sugars, thus becoming more enriched than their C source (Williams and Gordon, 1970; Hayes et al., 1989; Zohary et al., 1994; Briones et al., 1998; Lehmann et al., 2002; Jiao et al., 2010; Close and Henderson, 2020). The decrease in C:N ratios in the POM also reinforces this conclusion since secondary heterotrophic bacteria biomass generally have C:N between 4 and 5 (Lehmann et al., 2002), whereas residual degraded OM from primary producers would carry higher C:N signatures (van Mooy et al., 2002; Buchan et al., 2014). These latter signatures are not recorded by POM in the lower water columns of the lakes (Fig. 3).

The $\delta^{13}C_{DIC}$ signatures in La Preciosa and Alchichica are consistent with the mineralization of OM as they exhibit lower values below the oxycline than in surficial waters (Figs. 2 and 4). Similarly to what is observed in several other water bodies and notably stratified water columns such as the Black Sea (e.g. Fry et al., 1991), surface

610 photosynthesis increases $\delta^{13}C_{DIC}$ by fixing light DIC, while respiration transfers light OC back to the DIC pool at
611 depth. Such a decrease in $\delta^{13}C_{DIC}$ can also be seen in the oxycline of Lake La Alberca between 7 and 10 m.

612
613 *Influence of methanogenesis in Lake La Alberca de los Espinos*

614 La Alberca shows the least saline/alkaline water column and most peculiar geochemical depth profiles among the
615 four lakes. Notably, its [DIC] and $\delta^{13}C_{DIC}$ (the lowest of the studied lakes) increase from the lower metalimnion to
616 the hypolimnion, and further into the first cm of sediment porewaters, with $\delta^{13}C_{DIC}$ reaching almost 10 ‰ (Figs. 3;
617 4). The calculated CO_2 partial pressure (P_{CO2}) increases downward from slightly less than 1x $P_{CO2\text{-}atm}$ near the lake
618 surface up to almost 40x at the bottom of the lake (Table S2).

619 While the increase of [POC] at depth may contribute to the observed $\delta^{13}C_{DIC}$ increase, by mass balance, it should
620 also lower the [DIC] instead of increasing it. Similarly, the sinking of POC at depth followed by its
621 remineralization into DIC cannot explain these observations since it would lower the $\delta^{13}C_{DIC}$ in the hypolimnion
622 (Fig. 4). Overall, these observations require that a significant source of inorganic ^{13}C-rich carbon fuels the bottom
623 waters of La Alberca de los Espinos. The source of heavy carbon most likely results from methanogenesis, which
624 consumes organic carbon in the sediments and produces ^{13}C-depleted methane and ^{13}C-rich carbon dioxide
625 diffusing upward in the water column (i.e. acetoclastic methanogenesis, dominant in lacustrine contexts, Whiticar
626 et al., 1986). Methanogenesis, as an "alternative" OM remineralization pathway would be favored in La Alberca,
627 because it is relatively rich in OM (notably with high [DOC], Havas et al., submitted), and depleted in SO_4^{2-}
628 (Wittkop et al., 2014; Birgel et al., 2015; Cadeau et al., 2020) compared with the three other Mexican lakes. Based
629 on the $\delta^{13}C_{SOC}$ and porewater $\delta^{13}C_{DIC}$, we can tentatively calculate the methane isotopic signature in La Alberca
630 (see supplementary text S5). The resulting $\delta^{13}C_{CH4}$ in the first 10 cm of sediments is between -59 and -57 ‰, which
631 is consistent with the range of isotopic composition of methane after biogenic methanogenesis (Whiticar et al.,
632 1986).

633 Upward diffusing methane may be either (i) partly lost from the lake's surface (i.e. escaping the system) by
634 degassing or (ii) totally retained in the water column by complete oxidation (either abiotically by oxygenated
635 surface waters or biologically by methanotrophic organisms). The oxidation of CH_4 in the water column should
636 lead to the formation of ^{13}C-depleted carbon dioxide that would mix back with the lake DIC (and notably with
637 heavy methanogenic CO_2 produced at depth) and/or ^{13}C-depleted biomass (as POC or SOC) if it occurs through
638 methanotrophy. Thus, the net effect of combined methanogenesis and methane oxidation is expected to (i) generate
639 a $\delta^{13}C_{DIC}$ gradient from high to low values between the sediment porewaters and the oxycline as proposed
640 elsewhere (Assayag et al., 2008; Wittkop et al., 2014) and (ii) progressively lower sedimentary $\delta^{13}C_{SOC}$ in the case
641 of methanotrophy. Abiotic oxidation of methane by dioxygen is consistent with the observation that $\delta^{13}C_{DIC}$
642 decreases from porewaters (~ +10 ‰) to the oxycline (-4 ‰), reaching minimum values where dissolved-O_2 starts
643 to appear (Fig. 2). Microbial anaerobic oxidation of methane (AOM) could occur at the 17 m depth through Mn-
644 oxide reduction (Cai et al., 2021; Cheng et al., 2021) and possibly bacterial sulfate-reduction closer to the water-
645 sediment interface, as inferred for the surficial sediments of meromictic Lake Cadagno (Posth et al., 2017). Indeed,
646 we observe a net increase of particulate Fe and S concentrations at a depth of 25 m and a peak of solid sulfide
647 minerals in the surficial sediments (Fig. S5). However, $\delta^{13}C_{SOC}$ and $\delta^{13}C_{POC}$ are far from calculated $\delta^{13}C_{CH4}$,

suggesting that AOM is not a major process in the bottom lake waters and surface sediments (Lehmann et al., 2004) and thus that methanotrophy is not the main CH_4 oxidation pathway in Lake La Alberca.

Alternatively, if some portion of the methane escaped oxidation and degassed out of the lake, $\delta^{13}C_{DIC}$ would likely be driven to extreme positive values with time (Gu et al., 2004; Hassan, 2014; Birgel et al., 2015; Cadeau et al., 2020). This is not consistent with the average $\delta^{13}C_{DIC}$ in La Alberca (~ -3 ‰; Fig. 4), unless an additional counterbalancing source of DIC to this lake exists. This source of DIC could be volcanic CO_2-degassing (see section 5.1.1). Such a contribution may maintain the lake's average $\delta^{13}C_{total}$ close to a mantle isotopic signature and notably away from extreme positive values if CH_4-escape dominated. It is also possible that volcanic CO_2 degassing is coupled to methanogenesis by CO_2 reduction in addition to the acetoclastic type described above.

Although volcanic CO_2 could be an important source in the C mass balance of Lake La Alberca, we note that it cannot explain the very positive $\delta^{13}C_{DIC}$ in the sediment porewaters alone, thus bolstering the identification of methanogenesis. Importantly, this methane cycle is cryptic to the sediment record, as it is evidenced in the dissolved inorganic C phase, but not in the sedimentary organic matter or carbonates. This is a consequence of the lake's stratified nature, where the location of carbonate precipitation and methane production is decoupled.

Transfer of OM from the water column to the surficial sediments

The OC content in the first 12 cm of the sediment cores from the four lakes ranges from 1 to 13 wt. % (Table S3). This appears to be relatively elevated considering the predominantly autochthonous nature of OC and the oligotrophic conditions in these lakes (Alcocer et al., 2014; Havas et al., submitted). In Lake Alchichica, the recent OC burial flux in the sediment was estimated to represent between 15 and 26 $g.yr^{-1}.m^{-2}$ (Alcocer et al., 2014). This is within the range of values observed for small lakes around the world (Mulholland and Elwood, 1982; Dean and Gorham, 1998; Mendonça et al., 2017), though most of them receive allochthonous OM inputs. Different factors can favor the preservation of OM including lower respiration and oxidation rates due to anoxic bottom waters and scarce benthic biota and/or high sedimentation rates (Alcocer et al., 2014). Anaerobic respiration clearly occurs in the four lakes to some extent, as detailed for La Alberca, and as seen in the surficial sediment data of the other lakes as well (decreasing $\delta^{13}C_{DIC}$ in Alchichica, increasing C:N ratio in Atexcac and La Preciosa; Table S3). Nonetheless, the anoxic conditions prevailing in the hypolimnion most of the year are significantly more favorable to OM preservation than oxic conditions (Sobek et al., 2009; Kuntz et al., 2015). While the yearly mixing oxidizes most of the water column during the winter, it also generates a bloom of diatoms which fosters OM production (through shuttling up of bio essential nutrient such as N and Si) and development of anoxia (e.g. Adame et al., 2008). In Alchichica, the large size of some of the phytoplankton was also suggested to favor OM preservation (Adame et al., 2008; Ardiles et al., 2011). Because bacterial sulfate reduction (BSR) is a major remineralization pathway in SO_4-rich environments (e.g Jørgensen, 1982). the low sulfate content in La Alberca probably favors the preservation of high TOC in the sediments. Even though, appreciable BSR rates may occur in this lake (see discussion above and Fig. S5), similarly to other sulfate-poor environments due to rapid S-cycling (e.g. Vuillemin et al., 2016; Friese et al., 2021). Again, a complete mass-balance of these lakes C fluxes will be required to estimate their net C emission or sequestration behavior.

Although the nature and geochemical signatures of the OM that deposits in the sediments may vary throughout the year, it is interesting to infer from what part(s) of the water column surficial sedimentary OM comes during the stratified seasons. In the three lakes from the SOB, $\delta^{13}C_{SOC}$ and $(C:N)_{SOM}$ signatures of the surficial sedimentary OM lie somewhere between POM signatures from the upper water column and from the hypolimnion (Figs. 3, 4). More precisely, in Alchichica, the most surficial $\delta^{13}C_{SOC}$ and $(C:N)_{SOM}$ signatures (-25.7 ‰ and 10.4, respectively) are much closer to values recorded in the upper water column (~ -26.5 ‰ and 10.5, respectively), implying that the upper oxygenic photosynthesis production is primarily recorded. It is consistent with previous studies suggesting that most of the phytoplankton biomass being exported is composed of diatoms (Ardiles et al., 2011). In Lake Atexcac, however, $\delta^{13}C_{SOC}$ and $(C:N)_{SOM}$ signatures (~ -26.8 ‰ and 8, respectively) are closer to values recorded in the hypolimnion (~ -26.5 ‰ and 6.5, respectively) suggesting that SOM records mostly the anaerobic primary production.

In La Alberca, surficial $\delta^{13}C_{SOC}$ is markedly more negative (by ~ 2 to 3 ‰) than the deepest and shallowest water column values (Fig. 4), but close to what is recorded at the redoxcline depth of 17 m. However, the $(C:N)_{SOM}$ values are much higher than what is measured anywhere in the water column, which is consistent with OM remineralization by sulfate-reduction and methanogenesis in the sediments of this lake. Therefore, OM biogeochemical signatures in the surficial sediments of La Alberca could be strongly influenced by early diagenesis occurring at the water-sediment interface – despite favorable conditions for OM preservation.

Overall, this suggests that OM depositing at the bottom of these stratified lakes does not always record geochemical signatures from the same layers of the water columns and can be modified by very early diagenesis. It does not necessarily record the signatures of primary production by oxygenic photosynthesis from the upper column. For example, in Lake Atexcac, sedimentary OM records primary production by anoxygenic photosynthesis, even though POC concentration is highest in the upper water column. This highlights the diversity of geochemical signatures that can stem from continental environments despite their geographical, geological, and climatic proximity. A deeper understanding of the OM transfer process from water column to sediment will require more detailed analyses and comparison of the different OM pigments and molecules and could have strong implications for the interpretation of the fossil record in deep anoxic time.

6. CONCLUSIONS AND SUMMARY

The carbon cycles of four stratified alkaline crater lakes were described and compared based on the concentration and isotopic compositions of DIC and POC in the water columns and surficial (~10 cm) sedimentary carbonates and organic carbon. Overall our study shows the wide diversity of geochemical signatures found in continental stratified environments despite similar geological and climatic contexts. We identify different regimes of C cycling in the four lakes due to different biogeochemical reactions related to slight environmental and ecological variations. In more detail, we show that:

- External abiotic factors, such as the hydrological regime and the inorganic C sources in the lakes, control their alkalinity and thus, the buffering capacity of their waters. In turn, these differences in buffering capacity constrain variations in pH along the stratified water columns as well as the inorganic C isotope signatures recorded in the water columns and sediments of the lakes. The $\delta^{13}C_{carb}$ reflects the abiotic

factors generating the alkalinity gradient, but it is poorly representative of biological processes in lakes with high alkalinity. The external environmental factors further impact the C mass balance of the lakes with probable consequences on their net C-emitting or -sequestering status.

- Based on POC and DIC concentrations and isotopic compositions, combined with physico-chemical parameters, we are able to identify the activity of oxygenic photosynthesis and aerobic respiration in the four lakes studied. Anoxygenic photosynthesis and/or chemoautotrophy are also evidenced in two of the lakes, but their POC and DIC signatures can be equivocal.
- Methanogenesis is evidenced in the surficial sediments of the OM-rich Lake La Alberca de los Espinos and influences the geochemical signatures lower in the water column. However, it is recorded only in analyses of porewater dissolved species, but not imprinted in the sedimentary archives (OM and carbonates).
- The SOM geochemical signatures of these stratified lakes do not all record the same "biogeochemical layers" of the water column (e.g. anaerobic vs. aerobic metabolisms), and, in some cases, can be greatly modified by early diagenesis.

Author Contributions

RH and CT designed the study in a project directed by PLG, KB and CT. CT, MI, DJ, DM, RT, PLG and KB collected the samples on the field. RH carried out the measurements for C data; DJ the physico-chemical parameter probe measurements and EM provided data for trace and major elements. RH and CT analyzed the data. RH wrote the manuscript with important contributions of all co-authors.

Competing Interests

The authors declare that they have no conflict of interest.

Disclaimer

Acknowledgements

This work was supported by Agence Nationale de la Recherche (France; ANR Microbialites, grant number ANR-18-CE02-0013-02). The authors thank Anne-Lise Santoni, Elodie Cognard, Théophile Cocquerez and the GISMO platform (Biogéosciences, Université Bourgogne Franche-Comté, UMR CNRS 6282, France). We thank Céline Liorzou and Bleuenn Guéguen for the analyses at the Pôle Spectrométrie Océan (Laboratoire Géo-Océan, Brest, France) and Laure Cordier for ion chromatography analyses at IPGP (France). We thank Nelly Assayag and Pierre Cadeau for their help on the AP 2003 at IPGP.

References

Adame, M.F., Alcocer, J., Escobar, E., 2008. Size-fractionated phytoplankton biomass and its implications for the dynamics of an oligotrophic tropical lake. Freshw. Biol. 53, 22–31. https://doi.org/10.1111/j.1365-2427.2007.01864.x

761 Ader, M., Macouin, M., Trindade, R.I.F., Hadrien, M.-H., Yang, Z., Sun, Z., Besse, J., 2009. A
762 multilayered water column in the Ediacaran Yangtze platform? Insights from carbonate and organic
763 matter paired δ13C. Earth Planet. Sci. Lett. 288, 213–227. https://doi.org/10.1016/j.epsl.2009.09.024

764 Aharon, P., 2005. Redox stratification and anoxia of the early Precambrian oceans: Implications for
765 carbon isotope excursions and oxidation events. Precambrian Res. S0301926805000355.
766 https://doi.org/10.1016/j.precamres.2005.03.008

767 Alcocer, J., 2021. Lake Alchichica Limnology, Springer Nature. ed.

768 Alcocer, J., Ruiz-Fernández, A.C., Escobar, E., Pérez-Bernal, L.H., Oseguera, L.A., Ardiles-Gloria, V.,
769 2014. Deposition, burial and sequestration of carbon in an oligotrophic, tropical lake. J. Limnol. 73.
770 https://doi.org/10.4081/jlimnol.2014.783

771 Anderson, N.John., Stedmon, C.A., 2007. The effect of evapoconcentration on dissolved organic
772 carbon concentration and quality in lakes of SW Greenland. Freshw. Biol. 52, 280–289.
773 https://doi.org/10.1111/j.1365-2427.2006.01688.x

774 Ardiles, V., Alcocer, J., Vilaclara, G., Oseguera, L.A., Velasco, L., 2012. Diatom fluxes in a tropical,
775 oligotrophic lake dominated by large-sized phytoplankton. Hydrobiologia 679, 77–90.
776 https://doi.org/10.1007/s10750-011-0853-7

777 Armienta, M.A., Vilaclara, G., De la Cruz-Reyna, S., Ramos, S., Ceniceros, N., Cruz, O., Aguayo, A.,
778 Arcega-Cabrera, F., 2008. Water chemistry of lakes related to active and inactive Mexican volcanoes.
779 J. Volcanol. Geotherm. Res. 178, 249–258. https://doi.org/10.1016/j.jvolgeores.2008.06.019

780 Armstrong-Altrin, J.S., Madhavaraju, J., Sial, A.N., Kasper-Zubillaga, J.J., Nagarajan, R., Flores-Castro,
781 K., Rodríguez, J.L., 2011. Petrography and stable isotope geochemistry of the cretaceous El Abra
782 Limestones (Actopan), Mexico: Implication on diagenesis. J. Geol. Soc. India 77, 349–359.
783 https://doi.org/10.1007/s12594-011-0042-3

784 Assayag, N., Jézéquel, D., Ader, M., Viollier, E., Michard, G., Prévot, F., Agrinier, P., 2008. Hydrological
785 budget, carbon sources and biogeochemical processes in Lac Pavin (France): Constraints from δ18O
786 of water and δ13C of dissolved inorganic carbon. Appl. Geochem. 23, 2800–2816.
787 https://doi.org/10.1016/j.apgeochem.2008.04.015

788 Assayag, N., Rivé, K., Ader, M., Jézéquel, D., Agrinier, P., 2006. Improved method for isotopic and
789 quantitative analysis of dissolved inorganic carbon in natural water samples. Rapid Commun. Mass
790 Spectrom. 20, 2243–2251. https://doi.org/10.1002/rcm.2585

791 Bade, D.L., Carpenter, S.R., Cole, J.J., Hanson, P.C., Hesslein, R.H., 2004. Controls of δ13C-DIC in lakes:
792 Geochemistry, lake metabolism, and morphometry. Limnol. Oceanogr. 49, 1160–1172.
793 https://doi.org/10.4319/lo.2004.49.4.1160

794 Bekker, A., Holmden, C., Beukes, N.J., Kenig, F., Eglinton, B., Patterson, W.P., 2008. Fractionation
795 between inorganic and organic carbon during the Lomagundi (2.22–2.1 Ga) carbon isotope excursion.
796 Earth Planet. Sci. Lett. 271, 278–291. https://doi.org/10.1016/j.epsl.2008.04.021

797 Birgel, D., Meister, P., Lundberg, R., Horath, T.D., Bontognali, T.R.R., Bahniuk, A.M., de Rezende, C.E.,
798 Vasconcelos, C., McKenzie, J.A., 2015. Methanogenesis produces strong 13C enrichment in
799 stromatolites of Lagoa Salgada, Brazil: a modern analogue for Palaeo-/Neoproterozoic stromatolites?
800 Geobiology 13, 245–266. https://doi.org/10.1111/gbi.12130

Briones, E.E., Alcocer, J., Cienfuegos, E., Morales, P., 1998. Carbon stable isotopes ratios of pelagic and littoral communities in Alchichica crater-lake, Mexico. Int. J. Salt Lake Res. 7, 345–355. https://doi.org/10.1007/BF02442143

Buchan, A., LeCleir, G.R., Gulvik, C.A., González, J.M., 2014. Master recyclers: features and functions of bacteria associated with phytoplankton blooms. Nat. Rev. Microbiol. 12, 686–698. https://doi.org/10.1038/nrmicro3326

Cadeau, P., Jézéquel, D., Leboulanger, C., Fouilland, E., Le Floc'h, E., Chaduteau, C., Milesi, V., Guélard, J., Sarazin, G., Katz, A., d'Amore, S., Bernard, C., Ader, M., 2020. Carbon isotope evidence for large methane emissions to the Proterozoic atmosphere. Sci. Rep. 10, 18186. https://doi.org/10.1038/s41598-020-75100-x

Cai, C., Li, K., Liu, D., John, C.M., Wang, D., Fu, B., Fakhraee, M., He, H., Feng, L., Jiang, L., 2021. Anaerobic oxidation of methane by Mn oxides in sulfate-poor environments. Geology 49, 761–766. https://doi.org/10.1130/G48553.1

Callieri, C., Coci, M., Corno, G., Macek, M., Modenutti, B., Balseiro, E., Bertoni, R., 2013. Phylogenetic diversity of nonmarine picocyanobacteria. FEMS Microbiol. Ecol. 85, 293–301. https://doi.org/10.1111/1574-6941.12118

Carrasco-Núñez, G., Ort, M.H., Romero, C., 2007. Evolution and hydrological conditions of a maar volcano (Atexcac crater, Eastern Mexico). J. Volcanol. Geotherm. Res. 159, 179–197. https://doi.org/10.1016/j.jvolgeores.2006.07.001

Chako Tchamabé, B., Carrasco-Núñez, G., Miggins, D.P., Németh, K., 2020. Late Pleistocene to Holocene activity of Alchichica maar volcano, eastern Trans-Mexican Volcanic Belt. J. South Am. Earth Sci. 97, 102404. https://doi.org/10.1016/j.jsames.2019.102404

Cheng, C., Zhang, J., He, Q., Wu, H., Chen, Y., Xie, H., Pavlostathis, S.G., 2021. Exploring simultaneous nitrous oxide and methane sink in wetland sediments under anoxic conditions. Water Res. 194, 116958. https://doi.org/10.1016/j.watres.2021.116958

Close, H.G., Henderson, L.C., 2020. Open-Ocean Minima in δ13C Values of Particulate Organic Carbon in the Lower Euphotic Zone. Front. Mar. Sci. 7, 540165. https://doi.org/10.3389/fmars.2020.540165

Crowe, S.A., Katsev, S., Leslie, K., Sturm, A., Magen, C., Nomosatryo, S., Pack, M.A., Kessler, J.D., Reeburgh, W.S., Roberts, J.A., González, L., Douglas Haffner, G., Mucci, A., Sundby, B., Fowle, D.A., 2011. The methane cycle in ferruginous Lake Matano: Methane cycle in ferruginous Lake Matano. Geobiology 9, 61–78. https://doi.org/10.1111/j.1472-4669.2010.00257.x

Dean, W.E., Gorham, E., 1998. Magnitude and significance of carbon burial in lakes, reservoirs, and peatlands. Geology 26, 535. https://doi.org/10.1130/0091-7613(1998)026<0535:MASOCB>2.3.CO;2

Descolas-Gros, C., Fontungne, M., 1990. Stable carbon isotope fractionation by marine phytoplankton during photosynthesis. Plant Cell Environ. 13, 207–218. https://doi.org/10.1111/j.1365-3040.1990.tb01305.x

Emrich, K., Ehhalt, D.H., Vogel, J.C., 1970. Carbon isotope fractionation during the precipitation of calcium carbonate. Earth Planet. Sci. Lett. 8, 363–371. https://doi.org/10.1016/0012-821X(70)90109-3

Ferrari, L., Orozco-Esquivel, T., Manea, V., Manea, M., 2012. The dynamic history of the Trans-Mexican Volcanic Belt and the Mexico subduction zone. Tectonophysics 522–523, 122–149. https://doi.org/10.1016/j.tecto.2011.09.018

Fogel, M.L., Cifuentes, L.A., 1993. Isotope Fractionation during Primary Production, in: Engel, M.H., Macko, S.A. (Eds.), Organic Geochemistry, Topics in Geobiology. Springer US, Boston, MA, pp. 73–98. https://doi.org/10.1007/978-1-4615-2890-6_3

Friese, A., Bauer, K., Glombitza, C., Ordoñez, L., Ariztegui, D., Heuer, V.B., Vuillemin, A., Henny, C., Nomosatryo, S., Simister, R., Wagner, D., Bijaksana, S., Vogel, H., Melles, M., Russell, J.M., Crowe, S.A., Kallmeyer, J., 2021. Organic matter mineralization in modern and ancient ferruginous sediments. Nat. Commun. 12, 2216. https://doi.org/10.1038/s41467-021-22453-0

Fry, B., 2021. 13C/12C fractionation by marine diatoms 13.

Fry, B., Jannasch, H.W., Molyneaux, S.J., Wirsen, C.O., Muramoto, J.A., King, S., 1991. Stable isotope studies of the carbon, nitrogen and sulfur cycles in the Black Sea and the Cariaco Trench. Deep Sea Res. Part Oceanogr. Res. Pap. 38, S1003–S1019. https://doi.org/10.1016/S0198-0149(10)80021-4

Fulton, J.M., Arthur, M.A., Thomas, B., Freeman, K.H., 2018. Pigment carbon and nitrogen isotopic signatures in euxinic basins. Geobiology 16, 429–445. https://doi.org/10.1111/gbi.12285

Furian, S., Martins, E.R.C., Parizotto, T.M., Rezende-Filho, A.T., Victoria, R.L., Barbiero, L., 2013. Chemical diversity and spatial variability in myriad lakes in Nhecolândia in the Pantanal wetlands of Brazil. Limnol. Oceanogr. 58, 2249–2261. https://doi.org/10.4319/lo.2013.58.6.2249

Gérard, E., Ménez, B., Couradeau, E., Moreira, D., Benzerara, K., Tavera, R., López-García, P., 2013. Specific carbonate–microbe interactions in the modern microbialites of Lake Alchichica (Mexico). ISME J. 7, 1997–2009. https://doi.org/10.1038/ismej.2013.81

Gonzales-Partida, E., Barragan-R, R.M., Nieva-G, D., 1993. Analisis geoquimico-isotopico de las especies carbonicas del fluido geotermico de Los Humeros, Puebla, México. Geofis. Int. 32, 299–309.

Gröger, J., Franke, J., Hamer, K., Schulz, H.D., 2009. Quantitative Recovery of Elemental Sulfur and Improved Selectivity in a Chromium-Reducible Sulfur Distillation. Geostand. Geoanalytical Res. 33, 17–27. https://doi.org/10.1111/j.1751-908X.2009.00922.x

Gu, B., Schelske, C.L., Hodell, D.A., 2004. Extreme13C enrichments in a shallow hypereutrophic lake: Implications for carbon cycling. Limnol. Oceanogr. 49, 1152–1159. https://doi.org/10.4319/lo.2004.49.4.1152

Hassan, K.M., 2014. Isotope geochemistry of Swan Lake Basin in the Nebraska Sandhills, USA: Large 13C enrichment in sediment-calcite records. Geochemistry 74, 681–690. https://doi.org/10.1016/j.chemer.2014.03.004

Havig, J.R., Hamilton, T.L., McCormick, M., McClure, B., Sowers, T., Wegter, B., Kump, L.R., 2018. Water column and sediment stable carbon isotope biogeochemistry of permanently redox-stratified Fayetteville Green Lake, New York, U.S.A. Limnol. Oceanogr. 63, 570–587. https://doi.org/10.1002/lno.10649

Havig, J.R., McCormick, M.L., Hamilton, T.L., Kump, L.R., 2015. The behavior of biologically important trace elements across the oxic/euxinic transition of meromictic Fayetteville Green Lake, New York, USA. Geochim. Cosmochim. Acta 165, 389–406. https://doi.org/10.1016/j.gca.2015.06.024

Hayes, J.M., Popp, B.N., Takigiku, R., Johnson, M.W., 1989. An isotopic study of biogeochemical relationships between carbonates and organic carbon in the Greenhorn Formation. Geochim. Cosmochim. Acta 53, 2961–2972. https://doi.org/10.1016/0016-7037(89)90172-5

Hayes, J.M., Strauss, H., Kaufman, A.J., 1999. The abundance of 13C in marine organic matter and isotopic fractionation in the global biogeochemical cycle of carbon during the past 800 Ma. Chem. Geol. 161, 103–125. https://doi.org/10.1016/S0009-2541(99)00083-2

Henkel, J.V., Dellwig, O., Pollehne, F., Herlemann, D.P.R., Leipe, T., Schulz-Vogt, H.N., 2019. A bacterial isolate from the Black Sea oxidizes sulfide with manganese(IV) oxide. Proc. Natl. Acad. Sci. 116, 12153–12155. https://doi.org/10.1073/pnas.1906000116

Hurley, S.J., Wing, B.A., Jasper, C.E., Hill, N.C., Cameron, J.C., 2021. Carbon isotope evidence for the global physiology of Proterozoic cyanobacteria. Sci. Adv. 7, eabc8998. https://doi.org/10.1126/sciadv.abc8998

Iniesto, M., Moreira, D., Benzerara, K., Muller, E., Bertolino, P., Tavera, R., López-García, P., 2021a. Rapid formation of mature microbialites in Lake Alchichica, Mexico. Environ. Microbiol. Rep. 13, 600–605. https://doi.org/10.1111/1758-2229.12957

Iniesto, M., Moreira, D., Benzerara, K., Reboul, G., Bertolino, P., Tavera, R., López-García, P., 2022. Planktonic microbial communities from microbialite-bearing lakes sampled along a salinity-alkalinity gradient. Limnol. Oceanogr. lno.12233. https://doi.org/10.1002/lno.12233

Iniesto, M., Moreira, D., Reboul, G., Deschamps, P., Benzerara, K., Bertolino, P., Saghaï, A., Tavera, R., López-García, P., 2021b. Core microbial communities of lacustrine microbialites sampled along an alkalinity gradient. Environ. Microbiol. 23, 51–68. https://doi.org/10.1111/1462-2920.15252

Iñiguez, C., Capó-Bauçà, S., Niinemets, Ü., Stoll, H., Aguiló-Nicolau, P., Galmés, J., 2020. Evolutionary trends in RuBisCO kinetics and their co-evolution with CO2 concentrating mechanisms. Plant J. 101, 897–918. https://doi.org/10.1111/tpj.14643

Javoy, M., Pineau, F., Delorme, H., 1986. Carbon and nitrogen isotopes in the mantle. Chem. Geol., Isotopes in Geology—Picciotto Volume 57, 41–62. https://doi.org/10.1016/0009-2541(86)90093-8

Jézéquel, D., Michard, G., Viollier, E., Agrinier, P., Albéric, P., Lopes, F., Abril, G., Bergonzini, L., 2016. Carbon Cycle in a Meromictic Crater Lake: Lake Pavin, France, in: Sime-Ngando, T., Boivin, P., Chapron, E., Jezequel, D., Meybeck, M. (Eds.), Lake Pavin: History, Geology, Biogeochemistry, and Sedimentology of a Deep Meromictic Maar Lake. Springer International Publishing, Cham, pp. 185–203. https://doi.org/10.1007/978-3-319-39961-4_11

Jiao, N., Herndl, G.J., Hansell, D.A., Benner, R., Kattner, G., Wilhelm, S.W., Kirchman, D.L., Weinbauer, M.G., Luo, T., Chen, F., Azam, F., 2010. Microbial production of recalcitrant dissolved organic matter: long-term carbon storage in the global ocean. Nat. Rev. Microbiol. 8, 593–599. https://doi.org/10.1038/nrmicro2386

Jørgensen, B.B., 1982. Mineralization of organic matter in the sea bed—the role of sulphate reduction. Nature 296, 643–645. https://doi.org/10.1038/296643a0

Karhu, J.A., Holland, H.D., 1996. Carbon isotopes and the rise of atmospheric oxygen. Geology 24, 867. https://doi.org/10.1130/0091-7613(1996)024<0867:CIATRO>2.3.CO;2

Klawonn, I., Van den Wyngaert, S., Parada, A.E., Arandia-Gorostidi, N., Whitehouse, M.J., Grossart, H.-P., Dekas, A.E., 2021. Characterizing the “fungal shunt”: Parasitic fungi on diatoms affect carbon

flow and bacterial communities in aquatic microbial food webs. Proc. Natl. Acad. Sci. 118, e2102225118. https://doi.org/10.1073/pnas.2102225118

Knossow, N., Blonder, B., Eckert, W., Turchyn, A.V., Antler, G., Kamyshny, A., 2015. Annual sulfur cycle in a warm monomictic lake with sub-millimolar sulfate concentrations. Geochem. Trans. 16, 7. https://doi.org/10.1186/s12932-015-0021-5

Krissansen-Totton, J., Buick, R., Catling, D.C., 2015. A statistical analysis of the carbon isotope record from the Archean to Phanerozoic and implications for the rise of oxygen. Am. J. Sci. 315, 275–316. https://doi.org/10.2475/04.2015.01

Kuntz, L.B., Laakso, T.A., Schrag, D.P., Crowe, S.A., 2015. Modeling the carbon cycle in Lake Matano. Geobiology 13, 454–461. https://doi.org/10.1111/gbi.12141

Lehmann, M.F., Bernasconi, S.M., Barbieri, A., McKenzie, J.A., 2002. Preservation of organic matter and alteration of its carbon and nitrogen isotope composition during simulated and in situ early sedimentary diagenesis. Geochim. Cosmochim. Acta 66, 3573–3584. https://doi.org/10.1016/S0016-7037(02)00968-7

Lehmann, M.F., Bernasconi, S.M., McKenzie, J.A., Barbieri, A., Simona, M., Veronesi, M., 2004. Seasonal variation of the δC and δN of particulate and dissolved carbon and nitrogen in Lake Lugano: Constraints on biogeochemical cycling in a eutrophic lake. Limnol. Oceanogr. 49, 415–429. https://doi.org/10.4319/lo.2004.49.2.0415

Lelli, M., Kretzschmar, T.G., Cabassi, J., Doveri, M., Sanchez-Avila, J.I., Gherardi, F., Magro, G., Norelli, F., 2021. Fluid geochemistry of the Los Humeros geothermal field (LHGF - Puebla, Mexico): New constraints for the conceptual model. Geothermics 90, 101983. https://doi.org/10.1016/j.geothermics.2020.101983

Li, H.-C., Ku, T.-L., 1997. δ13C–δ18C covariance as a paleohydrological indicator for closed-basin lakes. Palaeogeogr. Palaeoclimatol. Palaeoecol. 133, 69–80. https://doi.org/10.1016/S0031-0182(96)00153-8

Logan, G.A., Hayes, J.M., Hieshima, G.B., Summons, R.E., 1995. Terminal Proterozoic reorganization of biogeochemical cycles. Nature 376, 53–56. https://doi.org/10.1038/376053a0

Lorenz, V., 1986. On the growth of maars and diatremes and its relevance to the formation of tuff rings. Bull. Volcanol. 48, 265–274. https://doi.org/10.1007/BF01081755

Lugo, A., Alcocer, J., Sánchez, Ma. del R., Escobar, E., Macek, M., 2000. Temporal and spatial variation of bacterioplankton abundance in a tropical, warm-monomictic, saline lake: Alchichica, Puebla, Mexico. SIL Proc. 1922-2010 27, 2968–2971. https://doi.org/10.1080/03680770.1998.11898217

Lugo, A., Alcocer, J., Sanchez, M.R., Escobar, E., 1993. Trophic status of tropical lakes indicated by littoral protozoan assemblages. SIL Proc. 1922-2010 25, 441–443. https://doi.org/10.1080/03680770.1992.11900159

Lyons, T.W., Reinhard, C.T., Planavsky, N.J., 2014. The rise of oxygen in Earth's early ocean and atmosphere. Nature 506, 307–315. https://doi.org/10.1038/nature13068

Macek, M., Medina, X.S., Picazo, A., Peštová, D., Reyes, F.B., Hernández, J.R.M., Alcocer, J., Ibarra, M.M., Camacho, A., 2020. Spirostomum teres: A Long Term Study of an Anoxic-Hypolimnion Population Feeding upon Photosynthesizing Microorganisms. Acta Protozool. 59, 13–38. https://doi.org/10.4467/16890027AP.20.002.12158

962 Mason, E., Edmonds, M., Turchyn, A.V., 2017. Remobilization of crustal carbon may dominate
963 volcanic arc emissions. Science 357, 290–294. https://doi.org/10.1126/science.aan5049

964 Mendonça, R., Müller, R.A., Clow, D., Verpoorter, C., Raymond, P., Tranvik, L.J., Sobek, S., 2017.
965 Organic carbon burial in global lakes and reservoirs. Nat. Commun. 8, 1694.
966 https://doi.org/10.1038/s41467-017-01789-6

967 Mercedes-Martín, R., Ayora, C., Tritlla, J., Sánchez-Román, M., 2019. The hydrochemical evolution of
968 alkaline volcanic lakes: a model to understand the South Atlantic Pre-salt mineral assemblages. Earth-
969 Sci. Rev. 198, 102938. https://doi.org/10.1016/j.earscirev.2019.102938

970 Milesi, V.P., Debure, M., Marty, N.C.M., Capano, M., Jézéquel, D., Steefel, C., Rouchon, V., Albéric, P.,
971 Bard, E., Sarazin, G., Guyot, F., Virgone, A., Gaucher, É.C., Ader, M., 2020. Early Diagenesis of
972 Lacustrine Carbonates in Volcanic Settings: The Role of Magmatic CO_2 (Lake Dziani Dzaha, Mayotte,
973 Indian Ocean). ACS Earth Space Chem. 4, 363–378.
974 https://doi.org/10.1021/acsearthspacechem.9b00279

975 Mook, W.G., Bommerson, J.C., Staverman, W.H., 1974. Carbon isotope fractionation between
976 dissolved bicarbonate and gaseous carbon dioxide. Earth Planet. Sci. Lett. 22, 169–176.
977 https://doi.org/10.1016/0012-821X(74)90078-8

978 Mulholland, P.J., Elwood, J.W., 1982. The role of lake and reservoir sediments as sinks in the
979 perturbed global carbon cycle. Tellus 34, 490–499. https://doi.org/10.1111/j.2153-
980 3490.1982.tb01837.x

981 O'Leary, M.H., 1988. Carbon Isotopes in Photosynthesis. BioScience 38, 328–336.
982 https://doi.org/10.2307/1310735

983 Pardue, J.W., Scalan, R.S., Van Baalen, C., Parker, P.L., 1976. Maximum carbon isotope fractionation
984 in photosynthesis by blue-green algae and a green alga. Geochim. Cosmochim. Acta 40, 309–312.
985 https://doi.org/10.1016/0016-7037(76)90208-8

986 Peiffer, L., Carrasco-Núñez, G., Mazot, A., Villanueva-Estrada, R.E., Inguaggiato, C., Bernard Romero,
987 R., Rocha Miller, R., Hernández Rojas, J., 2018. Soil degassing at the Los Humeros geothermal field
988 (Mexico). J. Volcanol. Geotherm. Res. 356, 163–174.
989 https://doi.org/10.1016/j.jvolgeores.2018.03.001

990 Petrash, D.A., Steenbergen, I.M., Valero, A., Meador, T.B., Pačes, T., Thomazo, C., 2022. Aqueous
991 system-level processes and prokaryote assemblages in the ferruginous and sulfate-rich bottom
992 waters of a post-mining lake. Biogeosciences 19, 1723–1751. https://doi.org/10.5194/bg-19-1723-
993 2022

994 Pimenov, N.V., Lunina, O.N., Prusakova, T.S., Rusanov, I.I., Ivanov, M.V., 2008. Biological fractionation
995 of stable carbon isotopes at the aerobic/anaerobic water interface of meromictic water bodies.
996 Microbiology 77, 751–759. https://doi.org/10.1134/S0026261708060131

997 Posth, N.R., Bristow, L.A., Cox, R.P., Habicht, K.S., Danza, F., Tonolla, M., Frigaard, N. -U., Canfield,
998 D.E., 2017. Carbon isotope fractionation by anoxygenic phototrophic bacteria in euxinic Lake
999 Cadagno. Geobiology 15, 798–816. https://doi.org/10.1111/gbi.12254

1000 Rendon-Lopez, M.J., 2008. Limnologia fisica del lago crater los Espinos, Municipio de Jiménez
1001 Michoacan.

1002 Ridgwell, A., Arndt, S., 2015. Chapter 1 - Why Dissolved Organics Matter: DOC in Ancient Oceans and
1003 Past Climate Change, in: Hansell, D.A., Carlson, C.A. (Eds.), Biogeochemistry of Marine Dissolved
1004 Organic Matter (Second Edition). Academic Press, Boston, pp. 1–20. https://doi.org/10.1016/B978-0-
1005 12-405940-5.00001-7

1006 Sackett, W.M., Eckelmann, W.R., Bender, M.L., Bé, A.W.H., 1965. Temperature Dependence of
1007 Carbon Isotope Composition in Marine Plankton and Sediments. Science 148, 235–237.
1008 https://doi.org/10.1126/science.148.3667.235

1009 Saghaï, A., Zivanovic, Y., Moreira, D., Benzerara, K., Bertolino, P., Ragon, M., Tavera, R., López-
1010 Archilla, A.I., López-García, P., 2016. Comparative metagenomics unveils functions and genome
1011 features of microbialite-associated communities along a depth gradient: Comparative metagenomics
1012 of microbialites from Lake Alchichica. Environ. Microbiol. 18, 4990–5004.
1013 https://doi.org/10.1111/1462-2920.13456

1014 Saini, J.S., Hassler, C., Cable, R., Fourquez, M., Danza, F., Roman, S., Tonolla, M., Storelli, N., Jacquet,
1015 S., Zdobnov, E.M., Duhaime, M.B., 2021. Microbial loop of a Proterozoic ocean analogue (preprint).
1016 Microbiology. https://doi.org/10.1101/2021.08.17.456685

1017 Satkoski, A.M., Beukes, N.J., Li, W., Beard, B.L., Johnson, C.M., 2015. A redox-stratified ocean 3.2
1018 billion years ago. Earth Planet. Sci. Lett. 430, 43–53. https://doi.org/10.1016/j.epsl.2015.08.007

1019 Schidlowski, M., 2001. Carbon isotopes as biogeochemical recorders of life over 3.8 Ga of Earth
1020 history: evolution of a concept. Precambrian Res. 106, 117–134. https://doi.org/10.1016/S0301-
1021 9268(00)00128-5

1022 Schiff, S.L., Tsuji, J.M., Wu, L., Venkiteswaran, J.J., Molot, L.A., Elgood, R.J., Paterson, M.J., Neufeld,
1023 J.D., 2017. Millions of Boreal Shield Lakes can be used to Probe Archaean Ocean Biogeochemistry.
1024 Sci. Rep. 7, 46708. https://doi.org/10.1038/srep46708

1025 Siebe, C., Guilbaud, M.-N., Salinas, S., Chédeville-Monzo, C., 2012. Eruption of Alberca de los Espinos
1026 tuff cone causes transgression of Zacapu lake ca. 25,000 yr BP in Michoacán, México. Presented at
1027 the IAS 4IMC Conference, Auckland, New Zeland, pp. 74–75.

1028 Siebe, C., Guilbaud, M.-N., Salinas, S., Kshirsagar, P., Chevrel, M.O., Jiménez, A.H., Godínez, L., 2014.
1029 Monogenetic volcanism of the Michoacán-Guanajuato Volcanic Field: Maar craters of the Zacapu
1030 basin and domes, shields, and scoria cones of the Tarascan highlands (Paracho-Paricutin region).
1031 Presented at the Pre-meeting field guide for the 5th international Maar Conference, Querétaro,
1032 México, pp. 1–37.

1033 Sigala, I., Caballero, M., Correa-Metrio, A., Lozano-García, S., Vázquez, G., Pérez, L., Zawisza, E., 2017.
1034 Basic limnology of 30 continental waterbodies of the Transmexican Volcanic Belt across climatic and
1035 environmental gradients. Bol. Soc. Geológica Mex. 69, 313–370.
1036 https://doi.org/10.18268/BSGM2017v69n2a3

1037 Silva Aguilera, R.A., 2019. Analisis del descenso del nivel de agua del lago Alchichica, Puebla, México
1038 120.

1039 Sirevag, R., Buchanan, B.B., Berry, J.A., Troughton, J.H., 1977. Mechanisms of C02 Fixation in Bacterial
1040 Photosynthesis Studied by the Carbon Isotope Fractionation Technique. Arch Microbiol 112, 4.

1041 Sobek, S., Durisch-Kaiser, E., Zurbrügg, R., Wongfun, N., Wessels, M., Pasche, N., Wehrli, B., 2009.
1042 Organic carbon burial efficiency in lake sediments controlled by oxygen exposure time and sediment
1043 source. Limnol. Oceanogr. 54, 2243–2254. https://doi.org/10.4319/lo.2009.54.6.2243

1044 Soetaert, K., Hofmann, A.F., Middelburg, J.J., Meysman, F.J.R., Greenwood, J., 2007. The effect of
1045 biogeochemical processes on pH. Mar. Chem. 105, 30–51.
1046 https://doi.org/10.1016/j.marchem.2006.12.012

1047 Talbot, M.R., 1990. A review of the palaeohydrological interpretation of carbon and oxygen isotopic
1048 ratios in primary lacustrine carbonates. Chem. Geol. Isot. Geosci. Sect. 80, 261–279.
1049 https://doi.org/10.1016/0168-9622(90)90009-2

1050 Thomas, P.J., Boller, A.J., Satagopan, S., Tabita, F.R., Cavanaugh, C.M., Scott, K.M., 2019. Isotope
1051 discrimination by form IC RubisCO from *Ralstonia eutropha* and *Rhodobacter sphaeroides* ,
1052 metabolically versatile members of ' *Proteobacteria* ' from aquatic and soil habitats. Environ.
1053 Microbiol. 21, 72–80. https://doi.org/10.1111/1462-2920.14423

1054 Ussiri, D.A.N., Lal, R., 2017. Carbon Sequestration for Climate Change Mitigation and Adaptation.
1055 Springer International Publishing, Cham. https://doi.org/10.1007/978-3-319-53845-7

1056 Van Mooy, B.A.S., Keil, R.G., Devol, A.H., 2002. Impact of suboxia on sinking particulate organic
1057 carbon: Enhanced carbon flux and preferential degradation of amino acids via denitrification.
1058 Geochim. Cosmochim. Acta 66, 457–465. https://doi.org/10.1016/S0016-7037(01)00787-6

1059 Vilaclara, G., Chávez, M., Lugo, A., González, H., Gaytán, M., 1993. Comparative description of crater-
1060 lakes basic chemistry in Puebla State, Mexico. SIL Proc. 1922-2010 25, 435–440.
1061 https://doi.org/10.1080/03680770.1992.11900158

1062 Vliet, D.M., Meijenfeldt, F.A.B., Dutilh, B.E., Villanueva, L., Sinninghe Damsté, J.S., Stams, A.J.M.,
1063 Sánchez-Andrea, I., 2021. The bacterial sulfur cycle in expanding dysoxic and euxinic marine waters.
1064 Environ. Microbiol. 23, 2834–2857. https://doi.org/10.1111/1462-2920.15265

1065 Vuillemin, A., Friese, A., Alawi, M., Henny, C., Nomosatryo, S., Wagner, D., Crowe, S.A., Kallmeyer, J.,
1066 2016. Geomicrobiological Features of Ferruginous Sediments from Lake Towuti, Indonesia. Front.
1067 Microbiol. 7. https://doi.org/10.3389/fmicb.2016.01007

1068 Wang, S., Yeager, K.M., Lu, W., 2016. Carbon isotope fractionation in phytoplankton as a potential
1069 proxy for pH rather than for [CO2(aq)]: Observations from a carbonate lake. Limnol. Oceanogr. 61,
1070 1259–1270. https://doi.org/10.1002/lno.10289

1071 Werne, J.P., Hollander, D.J., 2004. Balancing supply and demand: controls on carbon isotope
1072 fractionation in the Cariaco Basin (Venezuela) Younger Dryas to present. Mar. Chem. 92, 275–293.
1073 https://doi.org/10.1016/j.marchem.2004.06.031

1074 Whiticar, M.J., Faber, E., Schoell, M., 1986. Biogenic methane formation in marine and freshwater
1075 environments: CO2 reduction vs. acetate fermentation—Isotope evidence. Geochim. Cosmochim.
1076 Acta 50, 693–709. https://doi.org/10.1016/0016-7037(86)90346-7

1077 Williams, P.M., Gordon, L.I., 1970. Carbon-13: carbon-12 ratios in dissolved and particulate organic
1078 matter in the sea. Deep Sea Res. Oceanogr. Abstr. 17, 19–27. https://doi.org/10.1016/0011-
1079 7471(70)90085-9

Wittkop, C., Teranes, J., Lubenow, B., Dean, W.E., 2014. Carbon- and oxygen-stable isotopic signatures of methanogenesis, temperature, and water column stratification in Holocene siderite varves. Chem. Geol. 389, 153–166. https://doi.org/10.1016/j.chemgeo.2014.09.016

Zeyen, N., Benzerara, K., Beyssac, O., Daval, D., Muller, E., Thomazo, C., Tavera, R., López-García, P., Moreira, D., Duprat, E., 2021. Integrative analysis of the mineralogical and chemical composition of modern microbialites from ten Mexican lakes: What do we learn about their formation? Geochim. Cosmochim. Acta 305, 148–184. https://doi.org/10.1016/j.gca.2021.04.030

Zohary, T., Erez, J., Gophen, M., Berman-Frank, I., Stiller, M., 1994. Seasonality of stable carbon isotopes within the pelagic food web of Lake Kinneret. Limnol. Oceanogr. 39, 1030–1043. https://doi.org/10.4319/lo.1994.39.5.1030

Zyakun, A.M., Lunina, O.N., Prusakova, T.S., Pimenov, N.V., Ivanov, M.V., 2009. Fractionation of stable carbon isotopes by photoautotrophically growing anoxygenic purple and green sulfur bacteria. Microbiology 78, 757–768. https://doi.org/10.1134/S0026261709060137